ARTHROPOD SYSTEMATICS & PHYLOGENY

76 (2): 215–234
18.7.2018

SENCKENBERG

A new genus of eucerine bees endemic to southwestern North America revealed in phylogenetic analyses of the *Eucera* complex (Hymenoptera: Apidae: Eucerini)

Achik Dorchin *[1,2], Bryan Nicolas Danforth[1] & Terry Griswold[2]

[1] Department of Entomology, Cornell University, Ithaca, NY 14853, USA; Achik Dorchin * [adorchin@campus.haifa.ac.il]; Bryan Nicolas Danforth [bnd1@cornell.edu] — [2] USDA-ARS, Pollinating Insects Research Unit, Utah State University, Logan, UT 84322, USA; Terry Griswold [terry.griswold@ars.usda.gov] — * Corresponding author

Accepted 17.iii.2018.
Published online at www.senckenberg.de/arthropod-systematics on 29.vi.2018.
Editors in charge: Bradley Sinclair & Klaus-Dieter Klass

Abstract. The *Eucera* complex (Apidae: Eucerini), which traditionally included the genus *Eucera* and a few other related genera comprises a large complex in which generic boundaries have long remained unsettled. Based on comprehensive phylogenetic analyses, a recent study completely reorganized the generic classification of the group. Unexpectedly, both morphological and molecular analyses indicated that the taxon known as the *venusta*-group of the *Eucera* subgenus *Synhalonia* is in fact an isolated early diverging lineage, distantly related to *Synhalonia*. The only three species currently known in the *venusta*-group are endemic to arid and semi-arid habitats of the southwestern USA and Baja California in Mexico, and are relatively rare in entomological collections. Here we recognize a new genus: *Protohalonia* Dorchin **gen.n.**, compare its morphology with related genera, and present a revision and identification keys for the three species included. We reexamine the phylogenetic position of the new genus based on our previously published molecular and morphological datasets, which we supplement with data for the remaining *Protohalonia* species. All analyses recovered *Protohalonia* as a monophyletic group with strong support, sister to *Simanthedon* in the molecular and combined dataset analyses, or *Simanthedon* plus *Martinapis* in the morphological analysis; these taxa combined were sister to all the remaining lineages of the *Eucera* complex which together form the genus *Eucera*. Based on ancestral state reconstruction we identify unique traits supporting the monophyly of *Protohalonia* and document important diagnostic traits. Our results show that this taxon possesses a combination of apomorphic and plesiomorphic character states that appear in parallel in either the *Eucera* complex or outgroup taxa consistent with the phylogenetic position of the new genus. Lastly, we also propose replacement names for six new homonymies resulting from our recent classification of the *Eucera* complex.

Key words. Chihuahuan Desert, cladistics, classification, homoplasy, Mojave Desert, molecular phylogeny, pollinators, Sonoran Desert, systematics, taxonomy.

1. Introduction

The longhorn bee tribe Eucerini is a large tribe of solitary bees in the family Apidae, with ca. 780 species distributed over most regions of the world (Ascher & Pickering 2017). The Eucerini shows particularly high generic diversity in the Western Hemisphere of the world where various morphologically distinct lineages are found (Michener 2007; Praz & Packer 2014). Michener (2007: p. 708) highlighted the morphological similarity between some groups of Eucerini in the Old World and in North America, namely the genera *Eucera* Scopoli, 1770 and *Tetraloniella* Ashmead, 1899 (as reflected in his classification), and refrained from synonymizing these taxa in the absence of evidence on their phylogenetic relationships. Under Michener's (2007) classification, *Eucera* and other related genera (see below) comprise a large complex, including about half of the species in the Eucerini (390 species of the ca. 780 species according to Ascher & Pickering 2017), in which generic boundaries remained unresolved due to morphological intergradation among taxa.

Dorchin et al. (2018) presented comprehensive molecular and morphological analyses of the phylogenetic

relationships within this complex, referred to as the '*Eucera* complex'. Based on phylogenetic inference they proposed a complete reorganization of the generic classification of this clade, relegating most previously recognized genera, i.e., *Tetralonia* Spinola, 1839, *Xenoglossodes* Ashmead, 1899, *Cemolobus* Robertson, 1902, *Peponapis* Robertson, 1902, *Xenoglossa* Smith, 1854, and *Syntrichalonia* LaBerge, 1957, as subgenera within an expanded genus *Eucera* and synonymizing others (i.e., *Tetraloniella*, *Cubitalia* Friese, 1911) (Dorchin et al. 2018). Perhaps the most striking result from that study was the removal of the taxon known as the *venusta*-group of species from the valid *Eucera* subgenus *Synhalonia* Patton, 1879, and the recognition that it should form a separate new genus. Thus, three lineages were recognized within the *Eucera* complex: 1. the *venusta*-group; 2. the monotypic genus *Simanthedon* Zavortink, 1975; and 3. the genus *Eucera*, a group including all the remaining lineages (Dorchin et al. 2018).

The *venusta*-group currently includes only three known species restricted to arid and semi-arid habitats of the southwestern USA and adjacent Baja California in Mexico (see in 3.7.). Although all three species are rather uncommon in entomological collections in the USA, the *venusta*-group was relatively well studied in several revisions, perhaps due to its unusual morphology. It was first recognized as a distinct taxon by Timberlake (1961), who described two subspecies under the names *Tetralonia venusta* (Timberlake, 1961) (Figs. 1, 4, 17) and *Tetralonia venusta* ssp. *carinata* (Timberlake, 1961) (Figs. 2, 5, 18, 21) and recognized it as a "remarkably distinct and isolated species". The species originally placed in the genus *Synhalonia* (Patton 1879) were synonymized with the Old World genus *Tetralonia* (LaBerge 1957), and the genus name was later reinstated by Timberlake (1969). In his revision of the North American *Synhalonia*, Timberlake (1969) retained the *venusta*-group within *Synhalonia* even while presenting an illustration of the elaborate seventh sternite of the male, which strongly differs from that of any *Synhalonia* species but closely resembles that of *Martinapis* Cockerell, 1929 (a more distantly related taxon, outside the *Eucera* complex). In a later revision, Zavortink (1982) elevated *Synhalonia carinata* to species-level and added *Synhalonia amoena* Zavortink, 1982 (Figs. 3, 6, 19, 20) as a third species in the group. He listed various unusual features, such as the relatively short antennae and long first flagellomere of the male, and recognized the group as forming "a distinct element within *Synhalonia*". Michener (2000), who considered *Synhalonia* as a subgenus of *Eucera*, kept the *venusta*-group in *Synhalonia*, although he mentioned it as exceptional in his key to the North and Central American genera of Eucerini due to the unique structure of the female pygidial plate. Thus, despite identifying its unusual morphology, none of these authors considered the *venusta*-group as a separate taxon (see also list of synonyms in 3.5. for sequence of affiliation to genus).

Our recent molecular and morphological phylogenetic analyses suggest that the *venusta*-group is not at all closely related to *Synhalonia*, placing it in a much more distant position (Dorchin et al. 2018). Model-based analyses of the molecular and the combined molecular and morphological datasets recovered sister-relationships between the *venusta*-group and the monotypic genus *Simanthedon*, and between these two lineages combined and the remaining lineages of the genus *Eucera* (*sensu* Dorchin et al. 2018). Parsimony analyses of the morphological dataset also recovered the *venusta*-group as a distinct lineage sister to most *Eucera* lineages, but failed to recover the monophyly of either *Eucera* or the *Eucera* complex as a whole (Dorchin et al. 2018). Ancestral state reconstructions also performed in that study revealed a unique combination of morphological traits for the *venusta*-group, in both the male and the female sex, and highlighted one autapomorphy (Dorchin et al. 2018: table S5).

These unexpected molecular and morphological results were based on analyses including a single species from the *venusta*-group, *Eucera venusta* (Dorchin et al. 2018). Considering the important phylogenetic position of the group as an early diverging lineage, sister (together with *Simanthedon*) to all other *Eucera* complex lineages, examining the relationships among all members of the *venusta*-group and their closest relatives is much desired to validate a genus status for the group. In this study we: 1. complement our previous phylogenetic analyses with molecular sequence data and morphological data for the remaining species in the *venusta*-group: *Eucera carinata* and *E. amoena*; 2. compare the morphology of all species in the *venusta*-group and present an updated revision; and 3. recognize a valid genus status for the group and describe it as new to implement the classification changes implied by our recent and current phylogenetic results. Finally we propose replacement names to resolve five new homonyms created by our recently proposed classification (Dorchin et al. 2018) and a sixth existing homonym in the *Eucera* complex.

2. Methods

2.1. Morphological analyses

The external morphology of all species in the *venusta*-group was examined using pinned specimens, including the same individual vouchers used for DNA sequencing (see in 3.5.). The internal, structurally diverse genital complex and associated metasomal sternites of the males were dissected and cleared by submersion in NaOH overnight, and then glued onto white card stock for examination. Specimens were examined using a Leica M125 stereomicroscope with a Techniquip ProLine 80 LED ring light. A Keyence VHX-500F digital microscope was used at 30–200 × magnification to measure and take images of specimens. Images were edited using GIMP v2.8.18 (Kimball et al. 2016), and plates prepared using Inkscape v2.0 (Inkscape Development Team 2017).

For morphological analyses, we selected a subset of the taxa from the morphological matrix used in Dorchin et al. (2018) representing all the main clades and the morphological variation found within each of these clades. We favored taxa for which molecular data was obtained to match the taxon set used in molecular analyses (see in 2.2.). As outgroup we used one representative each from the genera *Ancyla* Lepeletier, 1841 and *Tarsalia* Morawitz, 1895 of the related tribe Ancylaini (*sensu* Michener 2007), and a total of 51 taxa from the tribe Eucerini (Table S1). To complete our morphological dataset, we scored character states for the two remaining species in the *venusta*-group, *Eucera carinata* and *E. amoena*. We used the 120-character matrix from Dorchin et al. (2018: supplementary material) with one new character (No. 121), the surface sculpture of the clypeus of the female, which appears in a unique state within the *venusta*-group (Table 2). It is described as follows: Female clypeus surface sculpture: (0) strongly irregularly rugosopunctate (as in Figs. 7, 8); (1) strongly punctate, at most weakly rugose (as in Fig. 9); (2) conspicuously punctate at least anteriorly; (3) with weak punctures or ridges. The corresponding character matrix is provided as Electronic Supplement file 1.

2.2. Molecular analyses

In molecular analyses we used the same taxa included in morphological analyses, which consist of a subset of the taxa from the molecular matrix of Dorchin et al. (2018) plus the two *venusta*-group species, *E. carinata* and *E. amoena* (Table S1). We obtained DNA for these uncommon species from pinned specimens deposited at the USDA/ARS, Pollinating Insects Research Unit, Logan, Utah (NPIC) (see list of specimens sequenced with Genbank accession numbers in Table S1). DNA was extracted from one to three legs and the rest of the specimens were preserved as vouchers. DNA was obtained using phenol-chlorophorm extractions following the methods described in Danforth (1999). PCR reactions were performed with HyTaq DNA polymerase (HyLabs) in a Biometra T1 thermocycler, with a blank sample as negative control. PCR products were examined visually using agarose gel electrophoresis, purified enzymatically using Exonuclease I and Alkaline Phosphatase, and sequencing was carried out by Hy Laboratories Ltd. (Rehovot, Israel), using BigDye Terminator v1.1 (Applied Biosystems), on the 3730xl DNA Analyzer with DNA Sequencing Analysis Software v.5.4. We used the six genes included in Dorchin et al. (2018): the nuclear protein coding genes RNA-polymerase II (hereafter Pol II, 841 bp), sodium potassium adenosine triphosphatase (NaK, 1441 bp), and LW-Rhodopsin (Opsin, 1156 bp), the ribosomal gene 28S (1556 bp), and the mitochondrial genes Cytochrome oxidase I (COI, 1318 bp) and Cytochrome b (Cytb, 433 bp). Because only pinned specimens with partly degraded DNA were available for *E. carinata* and *E. amoena*, rendering amplifications difficult, we only added new sequences of Opsin and COI, the most informative genes in previous phylogenetic analyses of the *Eucera* complex (Dorchin et al. 2018). We used the primer pairs mentioned in Dorchin et al. (2018), including the primers they designed to optimize amplification of the COI region and Opsin in the Eucerini. For this study, we designed two new sets of primers to amplify the long upstream fragment of Opsin (Table S2); however, we were unable to amplify the first 249 bases for *E. amoena* due to the low quality of the DNA. Chromatograms were trimmed, assembled and edited with Sequencher v5.4 for Macintosh (Gene Codes Corp.). Sequences were aligned using Mafft (Katoh & Standley 2013) and each alignment was corrected visually in Mesquite v3.02 (Maddison & Maddison 2015). A Chi-square test for heterogeneous base composition implemented in a beta version of Paup v4.0 (Swofford 2002) showed that only the mitochondrial COI and Cytb nt3 was significantly heterogeneous, we therefore excluded these bases from the phylogenetic analyses.

2.3. Phylogenetic analyses

Parsimony analyses of the morphological dataset were performed in TNT v1.1 (Goloboff et al. 2003, 2008) with the tree-bisection reconnection (TBR) swapping algorithm, using maximum length as the collapsing rule (collapsing rule 3). We performed analyses under equal weights with 500 replicates, holding 200 trees per replication. Node support was assessed using both Bremer supports (BSP) (Bremer 1994) and bootstrap support (BS) with 1000 replicates. For calculating BSP the 'suboptimal' value was increased stepwise by 1 and the tree buffer by 1000 at each step, to obtain accurate measures of support. A suboptimal value of 12 produced appropriate BSP values for all nodes of the strict consensus of all the most parsimonious trees. Analyses under implied weights were also performed using the same search parameters and different concavity constant values, from k = 1 up to the first k-value that gave the same topology as in the most parsimonious trees from our equal weights analysis. In this dataset k = 22 was the k value that produced the same tree topology as in the equal weights analysis (tree not presented) but trees under implied weighting were always shorter compared to those under equal weights.

In analyses of the molecular dataset, we first performed Maximum Likelihood (ML) analyses with Opsin and COI, the gene datasets to which we added new sequence data, separately (the significantly heterogeneous COI nt3 excluded), with the dataset partitioned by codon position (nt1, nt2, nt3), and with the Opsin introns in separate partition. The concatenated dataset (Opsin + Pol II + NaK + COI + Cytb + 28S) was then analyzed using five partitions: three partitions for each of the codon positions, and the Opsin introns and 28S in separate partitions. This analysis corresponds to the preferred analysis of Dorchin et al. (2018), namely the one that

produced the highest support values for morphologically recognized clades. Analyses were performed in RAxML v.8 (Stamatakis 2014) on the CIPRES server (Miller et al. 2010), using 1000 bootstrap replicates and applying GTR+G model to each partition. Because all parameters reached convergence with high ESS values (> 300) under the GTR+G model we did not explore simpler models. In analyses of the combined molecular and morphological analyses we added the morphological data as a separate multi-state ("MULTI") partition to our molecular dataset using the MK model (enforced by the "K-MK" command).

To study patterns of morphological trait evolution relative to the molecular phylogeny, we mapped the morphological characters onto our molecular phylogenetic tree and constructed their ancestral character states in Mesquite (Maddison & Maddison 2015) using the command "Trace character history" and parsimony as the construction method. WinClada v1.00.08 (Nixon 2002) was then used to visualize character state changes across the branches of the resulting tree using unambiguous character optimizations. In addition, we performed ML-based analyses of ancestral state construction in Mesquite with Mk1 as the probability model (Maddison & Maddison 2015). ML analyses are preferable for taking into account branch lengths and phylogenetic uncertainty, and were thus used to reexamine ancestral character states corresponding to particular diagnostic traits of the *venusta*-group that remained unresolved in parsimony-based analyses.

2.4. List of abbreviations

The morphological terminology used follows that of Michener (2007), including the following abbreviations: **S1**, **S2**, etc. – first, second, etc. metasomal sternites; **T1**, **T2**, etc. – first, second, etc. metasomal tergites. We used our own terminology to describe some important diagnostic components of the particularly complex sternite 7 of the male; the terms used are indicated in the figures.

Institutions from which material was examined are: **CAS** – California Academy of Sciences, San Francisco, California; **EMEC** – Essig Museum of Entomology, Berkley, California; **NPIC** – USDA/ARS, National Pollinating Insects Collection, Logan, Utah.

3. Results

3.1. Description and diagnosis of genus *Protohalonia*

Protohalonia Dorchin **gen.n.**

Type species. *Tetralonia venusta* Timberlake, 1961, by original designation.

Diagnosis. Unique characteristics of females of the genus *Protohalonia* within the Eucerini are: 1. clypeus moderately protuberant, strongly and irregularly rugosopunctate (Figs. 7, 8), and angulate anteriorly in profile (Figs. 10, 11); 2. pygidial plate narrowly cuneate and strongly elevated along midline (Fig. 12); and 3. scopal hairs of tibia and basitarsus fine and dense, unbranched (Figs. 13, 14); females can also be recognized by the fine and dense punctation of head (Fig. 15) and mesosoma and the long pubescence of the mesosoma and metasoma that completely conceals the underlying surface of mesoscutum (Fig. 16). Unique characteristics of males are: 1. pygidial plate narrow, tapering, delimited by complete marginal carina (Fig. 26), but the pygidial plate is variable, usually more broadly rounded apically, and with marginal carina interrupted preapically in *P. amoena* (Fig. 27); 2. S8 with conspicuous dorsal pubescence (Fig. 32); and 3. anterior lobe of lateral process of S7 strongly folded as seen in ventral view (Figs. 29, 31); males are also characterized by the following combination of traits: antennae moderately short, 3–3.6 × as long as compound eye; first flagellomere relatively long, maximum length about 0.6 to almost as long as second (Figs. 22, 23); elaborate medial process of S7, elongated and apically expanded to a broad, ventrally setose plate (Figs. 29–31); gonocoxa with posteromedial patch of sclerotized setae; and gonostylus gently arcuate as seen in lateral view (Fig. 34). In addition, both males and females can be easily separated from most genera of Nearctic and Neotropical Eucerini by the presence of 6 maxillary palpomeres, compared to five or less palpomeres in these other groups (exceptions: *Alloscirtetica* (Holmberg, 1903), *Eucera* (*Synhalonia*) and some species of *E.* (*Xenoglossodes*), *E.* (*Peponapis*), and *Gaesischia* Michener, LaBerge, and Moure, 1955).

Protohalonia are distinguished from subgenera of *Gaesischia* that have 6 maxillary palpomeres by the weak lower paraocular carina, appearing as a low ridge, and in the male, the simple gonostylus (Figs. 33, 34) and the above described antennal characteristics. They are further distinguished from *Martinapis* and *Melissodes* Latreille, 1825 by the convex anterolateral margin of the tegula; from *Florilegus* Robertson, 1900 by the obscured margin of the basitibial plate of the female, and the absence of an apical gradular spine of T7 of the male; and from most members of the genus *Svastra* Holmberg, 1884 by the lack of spatuloplumose hairs on the mesosoma and metasoma. Males can be separated from the

→ **Figs. 1–16.** Images to illustrate important diagnostic characters of females of *Protohalonia* Dorchin **gen.n.**: Habitus in lateral view of: **1**: *P. venusta*; **2**: *P. carinata*; **3**: *P. amoena*. Face in frontal view of: **4**: *P. venusta*; **5**: *P. carinata*; **6**: *P. amoena*. Clypeus in frontal view of: **7**: *P. venusta*; **8**: *P. amoena*; **9**: *Eucera* (*Syntrichalonia*) *fuliginea* (LaBerge, 1994). Clypeus in profile of: **10**: *P. venusta*; **11**: *P. amoena*. **12**: Tergite 6 with pygidial plate in dorsal view of *P. carinata*. Hind tibia and basitarsus showing pollen scopa and keirotrichiate area of: **13**: *P. venusta*, exterior view; **14**: *P. amoena*, interior view (ka – keirotrichiate area). **15**: Head in dorsal view of *P. amoena*. **16**: Mesosoma of female *P. amoena*.

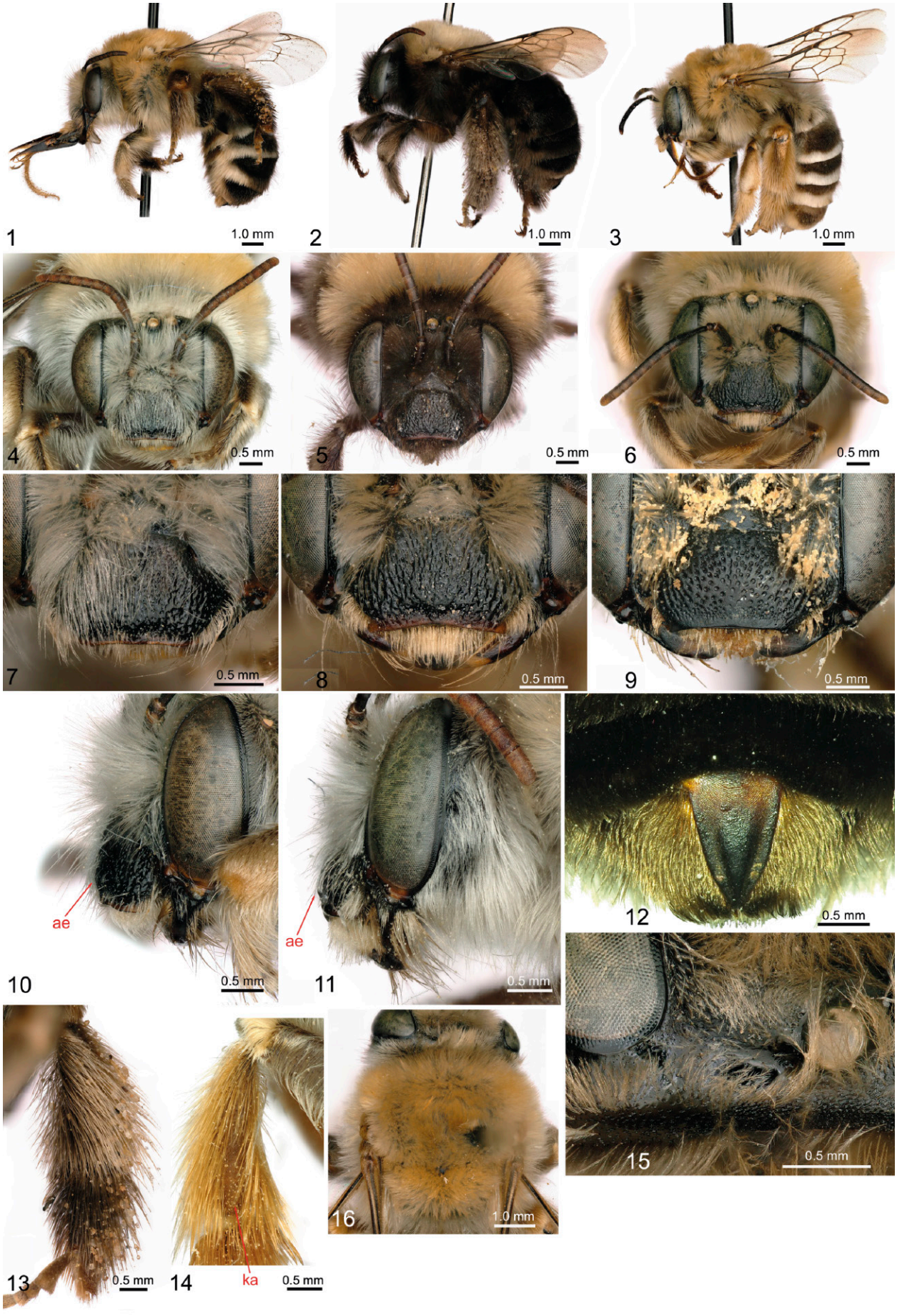
1
1.0 mm
2
1.0 mm
3
1.0 mm
4
0.5 mm
5
0.5 mm
6
0.5 mm
7
0.5 mm
8
0.5 mm
9
0.5 mm
ae
10
0.5 mm
ae
11
0.5 mm
12
0.5 mm
15
0.5 mm
16
1.0 mm
13
0.5 mm
14
ka
0.5 mm

related genus *Simanthedon* by the apically truncate clypeus, rounded terminal flagellomere, regularly broadened hind femur and tibia, and various structures of the genital complex. In addition to the unique structures of S7, S8, and the pygidial plate of the male listed above, males can be separated from most species in the genus *Eucera* by the simple, linearly oblique posterolateral carina of S6 (Fig. 28), which in *Eucera* is usually converging with an anterior carina, thus either curved basad or outward anteriorly (but various portions of the converging carinae are sometimes, probably secondarily, lost, see also in 3.2.).

Description. ***Female: Structure and distances****:* Medium size bees, body length 11–14.5 mm, forewing length 8–8.75 mm. Prestigma approximately as long as stigma. Marginal cell rounded distally, only slightly narrower than basally, well removed from costal margin. Three submarginal cells, second smallest, more or less quadrate, first about equal in size to third. First recurrent vein received at distal 1/3 or less of second submarginal cell, or sometimes interstitial with second submarginal crossvein. Jugal lobe of hind wing small, with distal edge not attaining, and usually much basal to vein cu-v. Clypeus moderately protuberant, in profile angulate anteriorly (Figs. 10, 11), produced in front of anterior tangent of compound eye by more than half, and less than 0.8 × width of compound eye, in frontal view slightly depressed submedially on each side, surface sculpture strongly and irregularly rugosopunctate (Figs. 7, 8). Proboscis moderately long, galeal blade about as long as compound eye, with surface sculpture microreticulate, shagreened or shiny. Maxillary palpus moderately long, about as long as mandible width at base, 6-segmented, segments 4–6 short, segments 5 and 6 together about as long as, or slightly longer than each of segment 2 or 3. Inner margin of compound eyes parallel sided (Figs. 4–6). Lower paraocular area without carina, at most with low ridge. Malar area linear, malar distance about equal to clypeocular distance, both approximately 0.1–0.15 × as long as mandible width at base. Vertex moderately short, ocelloccipital distance ¾ to about equal to one lateral ocellar diameter. Pygidial plate cuneate, strongly tapering distad to obtusely acute apex, with strongly elevated broad medial ridge (Fig. 12). ***Integument and vestiture****:* Integument of head and mesosoma dark, smooth, shiny, with fine punctures (Fig. 15). Vestiture long, densely pubescent, concealing completely most of underlying surface of head and mesosoma (Fig. 16), sparser, semi-erect basally on T1, shorter, decumbent, plumose on discs of following tergites (especially dense on usually concealed pregradular area). Vestiture coloration variable: dark brown to black in *P. carinata* (Figs. 2, 5); whitish, fulvous or light brown on head, mesosoma, and legs in *P. venusta* and *P. amoena* (Figs. 1, 3, 4, 6); dark brown or black on tergites with complete light apical band in *P. venusta* and *P. amoena* (Figs. 1, 3), in *P. venusta* varying from almost entirely dark to almost entirely white. Scopa with hairs unbranched, unusually fine, dense (Figs. 13, 14); keirotrichiate area small (Fig. 14). Basitibial plate obscured or almost completely obscured by pubescence in fresh specimens.

Male: Structure and distances*:* Body length 7–12 mm, forewing length 7–8 mm. Wing venation similar to female. Antenna moderately short, 3–3.6 × as long as compound eye, rounded in cross section, filiform, but weakly laterally compressed, crenate, and preapically transversely constricted in *P. carinata*. First antennal flagellomere moderately long, maximum length about 2/3 to almost as long as second (Figs. 22, 23). Structure of vertex, malar area, and clypeocular area as in female. Pygidial plate narrow, tapering distad, apically rounded with elevated median ridge and complete marginal carina (Fig. 26), (but see comment about variation in form of pygidial plate of *P. amoena* in *Diagnosis* above, and in Fig. 27). T6 with elevated lateral gradular spine, absent on T7. S6 with conspicuous basolateral marginal projection and linear posterolateral carina running obliquely on both sides parallel to sternal lateral margin, with no indication of anterior ridge (Fig. 28). Anterior lobe of lateral process of S7 rounded, ventrally concave with anterior edge strongly folded (Figs. 29, 31); posterior lobe with elevated transverse carina produced apicolaterally (Fig. 29), but faint, weakly indicated in *P. amoena* (Fig. 31). Medial process of S7 elaborate, with elongated arm curved apicomedially then apicolaterally, expanded apically into broad, ventrally setose plate (Figs. 29–31). S8 emarginate between rounded apical lobes, conspicuously pubescent posteriorly on dorsal surface (Fig. 32). Gonocoxa with patch of sclerotized setae posteromedially near attachment to gonostylus. Gonostylus longer than gonocoxa, gently arcuate in profile, with apex weakly expanded (Figs. 33, 34). ***Integument and vestiture****:* As in female, except as follows: Clypeus and labrum with light, whitish or pale-yellow maculation (Figs. 20, 21); clypeus with surface sculpture smooth (Figs. 20, 21); in *P. carinata* only vestiture of T3–T7 dark, vestiture of head, mesosoma, T1, and T2 light as in other species (Figs. 18, 21).

Etymology. The combining form "proto" of the new genus name, from the Greek word prôtos (meaning "first"), is joined with "halonia" referring to the genus-group name *Synhalonia* (Patton, 1879), on account of the early diverging phylogenetic position of this genus relative to that of *Synhalonia*, to which it was originally assigned. Gender feminine.

3.2. Key to genera of the *Eucera* complex

The genus *Protohalonia* does not run easily through the keys of Michener (2007) to Eucerini of North and Central America. It is included in *Eucera* (*Synhalonia*) but mentioned as exceptional in the key to females. In the key to males it runs either to *Peponapis* or *Synhalonia*, or even to a couplet including *Syntrichalonia* and *Svastra* (*Anthedonia*) (Michener, 1942), though it does not agree with these groups in one criterion or more. It is therefore necessary to present a modified key to facilitate identifi-

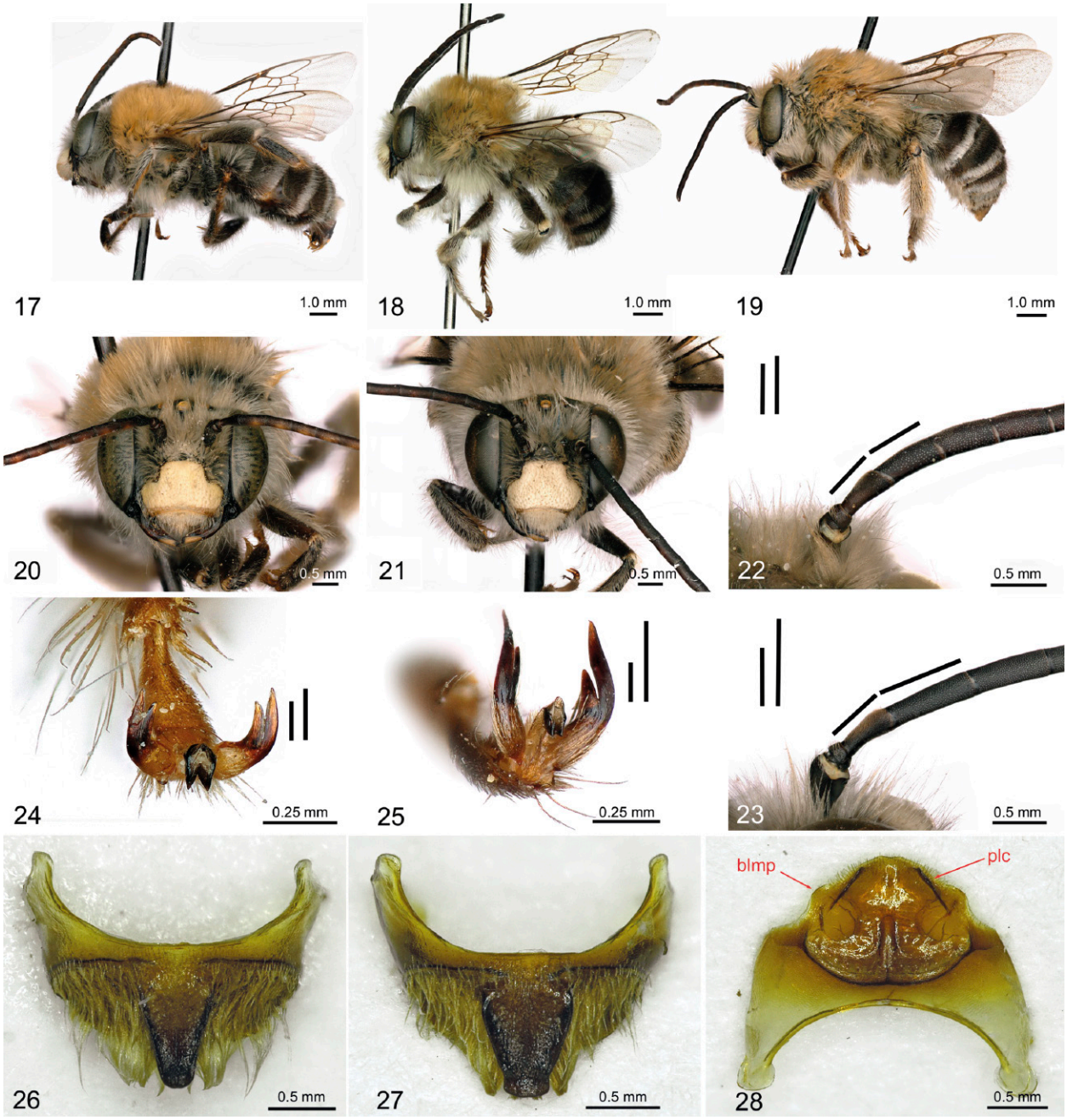

Figs. 17–28. Images to illustrate important diagnostic characters of males of *Protohalonia* Dorchin **gen.n.**: Habitus in lateral view of: **17**: *P. venusta*; **18**: *P. carinata*; **19**: *P. amoena*. Face in frontal view of: **20**: *P. amoena*; **21**: *P. carinata*. Base of antenna of: **22**: *P. amoena*; **23**: *P. carinata*. Hind claw of: **24**: *P.amoena*; **25**: *P. carinata*. Tergite 6 with pygidial plate in dorsal view of: **26**: *P. venusta*; **27**: *P. amoena*. **28**: Sternite 6 of *P. venusta* in ventral view (plc – posterolateral carina, blmp – basolateral marginal projection).

cation of the new genus among related genera. In the following key, modified from Michener (2007), genera of the *Eucera* complex, namely the Nearctic *Protohalonia* and *Simanthedon*, and *Eucera* of both the Old and the New World (Dorchin et al. 2018), are included and delineated from all Eucerini genera in the Nearctic region. Note that an apomorphy shared by most *Eucera* complex taxa is the presence of an elevated, heavily sclerotized carina on the posterior lobe of the lateral process of S7 of the male; this carina is usually linearly transverse (Fig. 28), but sometimes having the basal or apical portions reduced or modified.

1 Forewing with two submarginal cells (Palearctic) ..... ***Eucera* (*Eucera* s.str.)**

1' Forewing with three submarginal cells **2**

2 Stigma longer than prestigma (as in Michener 2007: fig. 112-4c); maxillary palpus short, 2- or 3-segmented; lateral gradular arm of T6 of female elevated, lamellate, and ended with a spine; commonly small species, 6.5–10 mm long, with appressed tan metasomal pubescence, without basal tergal hair bands (Neotropical to Texas) ..... ***Melissoptila* Holmberg, 1884**

2' Stigma as long as or shorter than prestigma (as in

Michener 2007: fig. 112-4b); maxillary palpus frequently longer, 3–6-segmented; T6 either with or without lateral gradular spine; mostly larger species, with variable metasomal vestiture **3**

3 Gradulus of S2 of female weakly biconvex, forming an angle of more than 140° between two convexities (as in Michener 2007: fig. 112-5a); pygidial plate of male unrecognizable; labrum long, 2/3–3/4 as long as broad; clypeocular distance long, at least as long as minimum diameter of first flagellar segment (Neotropical to Northern Mexico) ..... ***Thygater* Holmberg, 1884**

3' Gradulus of S2 of female usually more strongly biconvex, forming an angle of 140° or less between two convexities (as in Michener 2007: fig. 112-5b); pygidial plate of male discerned to various extents; labrum and clypeocular distance usually shorter ... **4**

4 Tegula narrowed anteriorly, anterolateral margin straight or concaved in anterior half or less (as in Michener 2007: fig. 112-8a); maxillary palpus usually 4-segmented, rarely 3-segmented; lateral gradular arm of T7 of male produced into a lateral gradular spine (North and South America) ..... ***Melissodes***

4' Tegula almost always with lateral margin convex (as in Michener 2007: fig. 112-8b); T7 of male usually not produced into a spine; *if* tegula narrowed anteriorly (as in *Martinapis*) *or* T7 of male with a lateral gradular spine (as in *Florilegus* and *Eucera* (*Xenoglossa*) *crassidentata* (Cockerell, 1949)) then maxillary palpus 5- or 6-segmented; maxillary palpus 4–6-segmented, rarely 3 segmented **5**

5 T2 basal hairband, and sometimes also T3, T4, and pubescence at scuto-scutellar boundary, with at least a few plumose and apically spatulate hairs (as in Michener 2007: fig. 112-10b); maxillary palpus 4- or 5-segmented; lateral gradular arm of T6 of female elevated, produced into a weak lateral gradular spine (Amphitropical American) ..... ***Svastra***

5' Spatuloplumose hairs absent on metasomal tergites and scutellum; maxillary palpus almost always 5- or 6-segmented; lateral gradular arm of T6 of female with or without a lateral gradular spine **6**

6 Female **7**

6' Male **14**

7 Basitibial plate with margin entirely exposed and surface often bare (as in Michener 2007: fig. 112-12a); T6 with a strong lateral gradular spine; metasomal tergites with weak iridescent reflection (Nearctic, Neotropical) ..... ***Florilegus***

7' Margin of basitibial plate almost always partly obscured by appressed hairs originating on disc (as in Michener 2007: fig. 112-12b); T6 without lateral gradular spine; metasomal tergites usually not iridescent **8**

8 Fore coxa with a conspicuous inner apical spine fringed with hairs (as in Michener 2007: fig. 112-13c) (Neotropical to Arizona) ..... ***Gaesischia* (in part)**

8' Fore coxa without spine **9**

9 Clypeus with margin indented at anterior tentorial pit to form almost right-angular notch (as in Michener 2007: fig. 112-13a); scopal hairs with minute barbs (Neotropical to Arizona) ..... ***Gaesischia* (*Gaesischiana*) Michener, LaBerge, and Moure, 1955 (in part)**

9' Clypeus with margin at level of anterior tentorial pits straight or slightly concave (as in Michener 2007: fig. 112-13b); scopal hairs usually either unbranched or conspicuously plumose **10**

10 Tibial spurs of middle leg short, less than half as long as distance from base of spur to anterior tibiofemoral articulation; lateral arm of hypostomal carina prominent, sublamelliform; T2 and T3 with broad basal bands of short white pubescence, contrasting with short, dark, appressed hairs posteriorly (Baja California, California) ..... ***Agapanthinus* LaBerge, 1957**

10' Tibial spurs of middle leg long, more than half as long as tibia; lateral arm of hypostomal carina weak, cariniform; vestiture of T2 and T3 variable, either with or without pale pubescent bands, or entirely covered by pale pubescence **11**

11 Tegula narrowed anteriorly, anterolateral margin concave (as in Michener 2007: fig. 112-8a); mandible strongly bidentate (but structure lost when the mandible worn), broadened apically thus nearly as wide preapically as basally (as in Michener 2007: fig. 112-14b) (Amphitropical American) ..... ***Martinapis***

11' Tegula not narrowed anteriorly, anterolateral margin convex (as in Michener 2007: fig. 112-8b); mandible rarely bidentate, usually pointed or scarcely notched at apex and much narrower preapically than basally (as in Michener 2007: fig. 112-14a) **12**

12 Pygidial plate strongly tapering and bluntly pointed apically (as in Fig. 12); clypeus moderately protuberant, produced in front of anterior tangent of compound eye in profile by 0.5–0.8 × eye width (Figs. 10, 11), slightly depressed submedially at each side; scopal hairs unbranched; keirotrichiate area small, its greatest width occupying less than half apical width of tibia (Fig. 14) **13**

12' pygidial plate broader, frequently rounded apically; *if* strongly tapering then either the clypeus flattened or only weakly convex, produced in front of anterior tangent of compound eye by ≤ 0.5 × eye width (as in Michener 2007: fig. 112-6b) *or* the keirotrichiate area larger, occupying at least half apical width of tibia (world-wide, except Australia) ..... ***Eucera* (in part)**

13 Pygidial plate strongly elevated along midline (Fig. 12); maxillary palpus 6-segmented; clypeus strongly irregularly rugosopunctate (Figs. 7, 8); vertex moderately short, ocelloccipital distance ¾ to about equal to one lateral ocellar diameter (southwestern deserts of the USA, California, Baja California) ..... ***Protohalonia***

13' Pygidial plate flattened; maxillary palpus 5-segmented; clypeus weakly sculptured, smooth; vertex

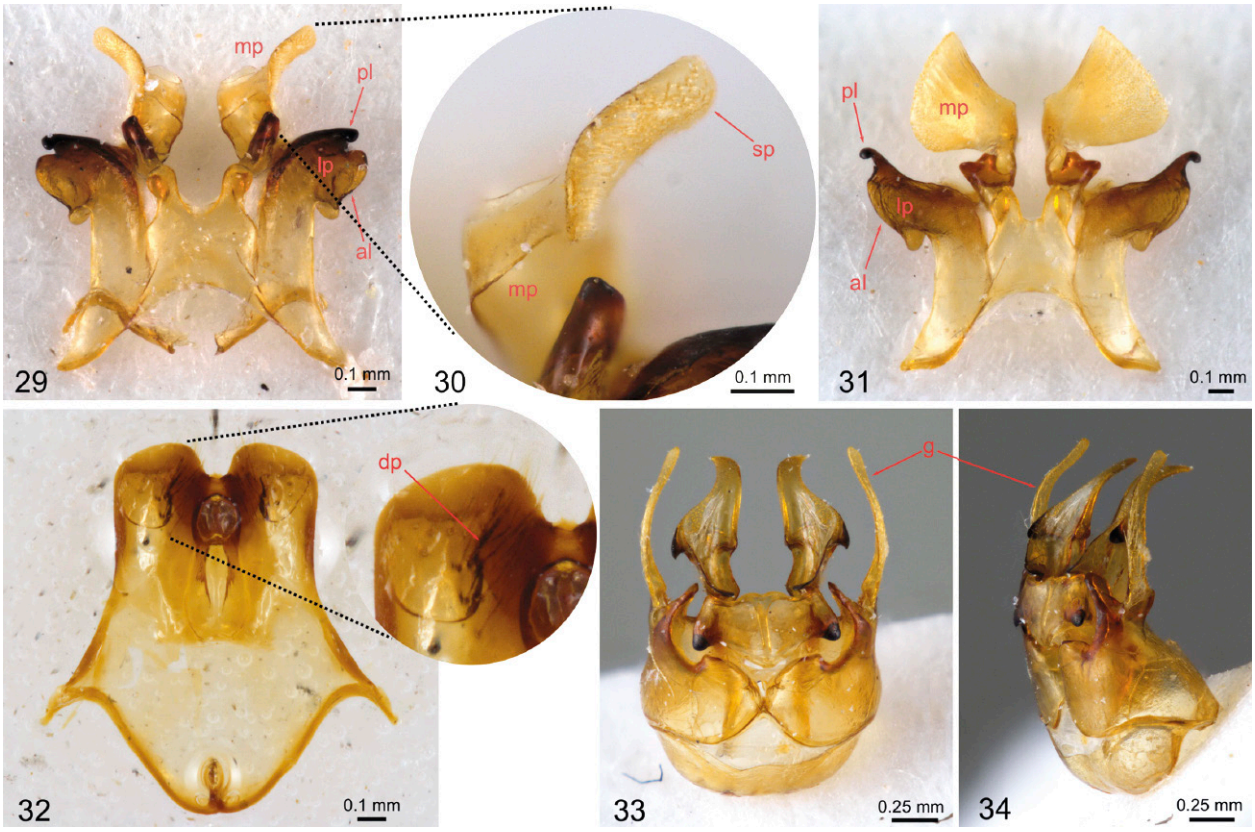

Figs. 29–34. Images to illustrate important diagnostic characters of males of *Protohalonia* Dorchin **gen.n.**: Sternite 7 in ventral view of: **29**, **30**: *P. venusta*; **31**: *P. amoena* (lp – lateral process, al – anterior lobe, pl – posterior lobe, mp – medial process, sp – setose plate). **32**: Sternite 8 of *P. venusta* (dp – dorsal pubescens). Genitalia of *P. carinata*: **33**: in dorsal view; **34**: in lateral view (g – gonostylus).

short, ocelloccipital distance ¼–⅓ lateral ocellar diameter (deserts of southwestern USA and Mexico) ..... ***Simanthedon***

14 Apex of terminal flagellomere pointed, hooked, and twisted slightly laterad (Baja California, California) ..... ***Agapanthinus***

14' Apex of terminal flagellomere rounded, straight **15**

15 S6 without posterolateral converging carinae, with elevated basal or medial area or median lamella (as in Michener 2007: fig. 112-10f); medial process of S7 elaborate, with a long curving arm extended posteriorly way beyond lateral process (as in Michener 2007: fig. 112-7i) **16**

15' S6 with posterolateral carina at each side (as in Fig. 28) often converging with anterior carina; sometimes only portions of the converging carinae present (as in Dorchin et al. 2018: fig. S2b,c), but median and basal areas unmodified, at most weakly convex, often weakly depressed; medial process of S7 often simple, at most shortly extending posteriorly beyond lateral process (as in Dorchin et al. 2018: fig. S2h,i,k) **17**

16 T7 with a lateral gradular spine; gonostylus short, robust, broadly expanded apically (as in Michener 2007: fig. 112-7g) (Nearctic, Neotropical) ..... ***Florilegus***

16' T7 without lateral gradular spine; gonostylus long and slender, not or scarcely expended apically (Neotropical to Arizona) ..... ***Gaesischia* (in part)**

17 Hind femur modified, enlarged with area of short, dense hairs near bare undersurface of posterior margin; flagellum tapering, terminal flagellomere compressed and sometimes expanded (Neotropical, Arizona) ..... ***Gaesischia* (*Gaesischiana*)**

17' Hind femur more slender; flagellum usually unmodified, rarely terminal flagellomere dorsoventrally compressed (as in *Eucera* (*Cemolobus*)) **18**

18 Clypeus apically reflexed, snout-like, forming distinct preapical angle in profile (as in Michener 2007: fig. 112-6g); S5 with thick tufts of hairs arising at shallow submedial emarginations on both sides, oriented posteromedially; hind femur slender, rounded in cross section (deserts of southwestern USA and Mexico) ..... ***Simanthedon***

18' Clypeus uniformly convex or straight, at most slightly depressed preapically, then weakly sinuate in profile (as in *Eucera* (*Cemolobus*)); S5 simple, usually without tufts of hairs; hind femur regularly robust, with lower posterior margin obtusely carinate, thus bluntly angular in cross section **19**

19 S6 with oblique posterolateral carina linear, neither converging with anterior carina or ridge (as in Fig. 28) nor joined with anterolateral branch carina re-

flecting an anterolateral angle or lobe; medial process of S7 elaborate, with a long curving arm extended posteriorly way beyond lateral process and produced apically into a broad ventrally setose plate (as in Figs. 29–31); antennae moderately short, 3–3.6 × as long as compound eye **20**

19' S6 variable: oblique posterolateral carina often converging with, or accompanied by anterior carina, and curved basad anteriorly (as in Dorchin et al. 2018: fig. S2b) *or* curved outward, thickened basally, and joined with a lateral branch carina reflecting an anterolateral angle or lobe (as in Dorchin et al. 2018: fig. S2c), although sometimes the converging carinae almost completely absent but a lateral branch is present (as in Dorchin et al. 2018: fig. S2d); medial process of S7 usually simple, at most shortly extending posteriorly beyond lateral process (as in Dorchin et al. 2018: fig. S2h,i,k); antennae short to long, often more than 3.6 × as long as compound eye (worldwide, except Australia) ..... ***Eucera* (in part)**

20 Pygidial plate narrow with an elevated longitudinal ridge, and apically rounded (Figs. 26, 27); spine of front tibial spur shorter than velum bearing shaft; gonostylus simple, uniformly covered with sparse setae (Figs. 33, 34); S8 dorsally pubescent (Fig. 32) (southwestern deserts of USA, California; Mexico, Baja California) ..... ***Protohalonia***

20' Pygidial plate broad, flattened, and apically truncate; spine of front tibial spur longer than velum bearing shaft; gonostylus elaborate with a broad anterior lobe completely obscured by dense setae, and with attenuate posterior lobe; S8 hairless except for a few isolated hairs on apical margin (as in Dorchin et al. 2018: fig. S2m) (Amphitropical American) ..... ***Martinapis***

3.3. Species-level revision

Our character exploration found a suite of diagnostic characters for each of the *Protohalonia* species (Table 2). Females of *P. carinata* are most readily identified by their darker vestiture, dark brown to black except lighter brown on dorsal parts of mesosoma and sometimes also basally on T1 (Figs. 2, 5), and the hairs on metasomal tergites sparse enough to expose the underlying integument. Females of this species are additionally distinguished by the stipital comb teeth widely separated (space between teeth about twice the basal diameter of adjacent comb teeth), and have ordinary branched hairs apicomedially on the underside of their mesosoma. Males of *P. carinata* can be separated from other *Protohalonia* species by the slightly longer crenate antenna, sinuate in lateral view, the terminal flagellomere transversely constricted preapically, and first flagellomere distinctly shorter than the second (Fig. 23). In contrast, in females of both *P. amoena* and *P. venusta* the head, mesosoma, and basal leg segments are covered with light pubescence (Figs. 1, 3, 4, 6), the metasoma has dense posterior hair bands, the stipital comb teeth space is less than half that described above, and the medial underside of the mesosoma has modified, unbranched apically bent hairs; the males have shorter and filiform antennae, with the terminal flagellomere regularly rounded, and the first flagellomere almost as long as second (Fig. 22).

Separating *P. amoena* and *P. venusta* is more difficult with the naked eye, but both sexes exhibit a number of structural differences. The male of *P. amoena* differs from both *P. venusta* and *P. carinata* in: the usually apically broader pygidial plate, with lateral carina weakly interrupted before apex (Fig. 27); the slightly less protuberant clypeus, weakly angular and submedially depressed on both sides; and structures of the genitalia and associated sternites (Table 2), most distinctly the greatly enlarged apical lobe of medial process of S7 (Fig. 31). The females can be separated based on the lighter scopa, especially the bright ferruginous hairs on the inner side of basitarsus; coarse surface sculpture of the clypeus, coarsely rugusopunctate (Fig. 8), and strongly angulate anteriorly in profile; and dense light tergal hair bands, that of T2 concealing completely the underlying integument in fresh specimens. In contrast, in males of both *P. venusta* and *P. carinata*: the pygidial plate is narrowly rounded apically, with complete lateral carina (Fig. 26); the clypeus is slightly more protuberant and rounded; and among other structural differences of the genital complex (Table 2), the smaller apical lobe of the medial process of S7 (Fig. 29). The female of *P. venusta* has an overall slightly darker scopa, particularly brownish ferruginous to black on the inner side of the basitarsus; the clypeus is usually less strongly sculptured (Fig. 7); and the tergal hairband on T2 sparser medially, not concealing the underlying surface even in fresh specimens.

3.4. Key to species of the genus *Protohalonia*

The three known species of *Protohalonia* **gen.n.** can be determined using the following key:

1 Female **2**

1' Male **4**

2 Vestiture of head, sides and underside of mesosoma, legs, and T2–4 uniformly dark brown to black (Figs. 2, 5), rarely the mesosoma light and T2–4 with a narrow light band at marginal zone (as observed in a specimen from Baja California), that on T2 never concealing the underlying integument; mesosoma with ordinary branched hairs on ventral side; stipital comb teeth widely spaced, separated by about 2 basal diameters of adjacent comb teeth (cismontane California to Baja California) ..... ***Protohalonia carinata***

2' Vestiture of head, mesosoma, and basal leg segments light (Figs. 1, 3, 4, 6), and T2–4 almost entirely light or with a broad light band at marginal zone, *if* tergites almost entirely dark then apical bands of T2–5 with at least some light hairs at lateral extremities,

that on T2 always concealing the underlying integument at least laterally (Figs. 1, 3); mesosoma with unbranched apically bent hairs posteromedially on ventral side; stipital comb teeth closely packed, separated by less than 1 basal diameter of adjacent comb teeth **3**

3 Scopal hair pale grey to brown on outer surface of tibia, brownish ferruginous to black on inner side of basitarsus; apical fascia of T2 not as dense medially and does not conceal underlying integument even in fresh specimens (Arizona to California, southern Oregon, and Baja California) .... ***Protohalonia venusta***

3' Scopal hair cream whitish on outer surface of tibia, bright ferruginous on inner side of basitarsus; T2 with dense apical fascia concealing completely underlying integument (southwestern deserts from New Mexico to southern California) ..... ***Protohalonia amoena***

4 Antenna long, about 3.6 × as long as compound eye, weakly laterally compressed, weakly crenate thus sinuate in lateral view; maximum length of first antennal flagellomere 0.6–0.7 × as long as second (Fig. 23); terminal flagellomere transversely constricted before apex; outer ramus of hind claw distinctly longer than inner ramus (Fig. 25) (cismontane California to Baja California) ..... ***Protohalonia carinata***

4' Antennae short, about 3.0 × as long as compound eye, rounded in cross section, filiform; maximum length of first antennal flagellomere more than 0.8 × as long as second (Fig. 22); terminal flagellomere uniformly broad; outer ramus of hind claw only slightly longer than inner ramus (Fig. 24) **5**

5 Pygidial plate narrowly rounded at apex with complete lateral carina (Fig. 26); lateral process of S7 with a large, strongly carinate posterior lobe, and with a short apicolateral spine (Fig. 29); distal arm of medial process of S7 curved dorsally apicomesad from a sclerotized dark angle, and produced apically into a broad oval lobe (Fig. 29) (Arizona to California, southern Oregon, and Baja California) ..... ***Protohalonia venusta***

5' Pygidial plate usually more broadly rounded at apex with lateral carina weakly interrupted before apex (Fig. 27); lateral process of S7 with a small posterior lobe with faint carina and a long, hooked apicolateral spine (Fig. 31); distal arm of medial process of S7 curved ventrally apicomesad from a sclerotized dark angle, and produced apically into a greatly enlarged, fan-shaped lobe (Fig. 31) (southwestern deserts from New Mexico to southern California) ..... ***Protohalonia amoena***

3.5. Material examined

Protohalonia venusta (Timberlake, 1961) comb.n.

Tetralonia venusta ssp. *venusta* Timberlake, 1961: 209–12.
Synhalonia venusta ssp. *venusta*; Timberlake 1969: 1–76.
Eucera (*Synhalonia*) *venusta*; Michener 2000: chapter 112.

Holotype ♀, 'Shoshone, 9.6 mi. | N., Inyo Co. | Calif.[ornia] V-3-60', 'Oe.[nothera] Clavaeformis | var. aurantiaca', 'J. W. MacSwain | collector', 'HOLOTYPE <red label> | T. venusta', '620', 'Tetralonia venusta type Timb.[erlake]', 'California Academy of Sciences | Type No. 14879' <hind legs and metasoma detached, basal parts damaged by pests placed in separate tube labeled 'California Academy of Sciences Type No. 14879'> (CAS). – Paratype ♂, 'Dissection No. | 810915-5 | T. J. Zavortink', 'Shoshone, 9.6 mi. | N., Inyo Co. | Calif.[ornia] V-3-60', 'Oe.[nothera] Clavaeformis | var. aurantiaca', 'J. W. MacSwain | collector', '614', 'Paratype | T. venusta', 'UC Berkeley | EMEC | 1134420' <S6–8 and genitalia in separate tube labeled 'Dissection No. 810915-5 T. J. Zavortink> (EMEC). – Paratype ♂, 'Dissection No. | 810915-3 | T. J. Zavortink', '3mi. N. Big Pine | Inyo Co. Calif.[ornia] | 27-v-59', 'Oe.[nothera] Clavaeformis | var. cruciformis', 'P.H. Raven | Collector', '1810', 'Paratype | S. venusta', 'Synhalonia venusta | (Timb.) [erlake] | T. J. Zavortink | Det. 1981', 'UC Berkeley | EMEC | 1134419' <S6–8 and genitalia in separate tube labeled 'Dissection No. 810915-3 T. J. Zavortink> (EMEC). – Paratype ♀, 'Hopkins Well | Riverside Co., | Calif.[ornia] iv-27-49', LW Quate | Collector', 'Paratype | T. venusta', 'UC Berkeley | EMEC | 1134545' (EMEC). – Paratype ♀, '18 miles W. of | Blythe, Cal[ifornia]' <Riverside Co., Hopkins Well according to Timberlake (1961)>, 'On Oenothera | clavaeformis', 'Timberlake | Coll.[ector] ap[ril] <text not clear> 17 [19]58', 'Paratype | T. venusta', 'Synhalonia | venusta | Timb.[erlake] det. <unclear text>', 'UC Berkeley | EMEC | 1134544' (EMEC). ♀, USA, California, Riverside Co., 18 mi [29 km] W of Blythe, 13.iv.2016, Orr leg., at *Psorothamnus emoryi*, T. Griswold det. (NPIC). ♀, USA, Arizona, Yuma Co., 22 mi [35.4 km] SE of Salome, 31.iv.1973, at *Larrea divaricata* [*L. tridentata*], T. Griswold det. (NPIC). 3♀, USA, Arizona, Yuma Co., 22 mi SE of Salome, vi.1973, Bohart leg., at *Larrea* sp. [*L. tridentata*], W. E. LaBerge det. (NPIC). ♀, USA, Nevada, Clark Co., 2.3 mi [3.7 km] E of Sheep Mt., 2939 ft [896 m], 12.v.2004, Griswold & Ahlstrom leg., blue pan trap, A. Dorchin det. 2015 (NPIC). ♂, USA, Nevada, Clark Co., Riverside, 11/21.v.1983, Parker leg., T. Griswold det. 1989 (NPIC). ♀, USA, Nevada, Washoe Co., Gerlach, 29.v.1939, Ting, Cazier, Downes & Aitken leg. (EMEC). ♂, USA, Oregon, Harney Co., 10.7 mi [17.2 km] S of Fields, 17.vi.1962, Stage leg., at *Oenothera clavaeformis* var. *integrior*, Zavortink det. (EMEC).

Protohalonia carinata (Timberlake, 1961) comb.n.

Tetralonia venusta ssp. *carinata* Timberlake, 1961: 209–12.
Synhalonia venusta ssp. *carinata*; Timberlake 1969: 1–76.
Synhalonia carinata; Zavortink 1982: 19–25.
Eucera (*Synhalonia*) *carinata*; Michener 2000: chapter 112.

Holotype ♂, 'Pinnacles, | Calif.[ornia] | San Benito Co. | [19.] v.19.41' <date according to Timberlake 1961>, 'J. W. MacSwain | collector', 'HOLOTYPE | T. carinata', 'Tetralonia venusta carinata | Type Timb.[erlake]', 'California Academy of Sciences | Type No. 14880' <S7,8 and genitalia dissected and glued onto card under specimen, many parts damaged or missing> (CAS). – ♀, USA, California, San Benito Co., 2 km NW by N of Scout Peak, 430 m, 3.vi.2011, Lamperty leg., at *Clarkia unguiculata*, T. Griswold det. (NPIC); 2♂, USA, California, San Benito Co., S of Hernandez, 22.v.1996, Griswold leg., T. Griswold det. (NPIC); ♂, USA, California, Madera Co., S of South Fork, 26.v.1996, Griswold leg., at *Lotus scoparius*, T. Griswold det. (NPIC); ♀, USA, California, Mariposa Co., Eagle Peak, 1.1 mi [1.7 km] S of El Portal, 286 m, 15.vii.2005, Briggs leg., at *Clarkia williamsonii*, K. T. Huntzinger det. (NPIC); ♀, USA, California, Mariposa Co., Eagle Peak, 1.1 mi [1.7 km] S of El Portal, 286 m, 27.vii.2005, Ikerd leg., in blue pan trap, T. Griswold det. (NPIC); ♀, USA, California, Mariposa Co., 1.1 mi [1.7 km] E by S of Half Dome, 1994 m, 23.v.2005, Stephens leg., T. Griswold det. (NPIC); 3♂, USA, California, Mariposa Co., Foresta Rd., 1.1 mi [1.7 km] S Eagle Peak, 576 m, 5.v.2004, Ikerd & Briggs leg., at *Clarkia unguiculata*, *Gilia capitata* ssp. *Medio-*

montana, T. Griswold det. (NPIC); 3♂, ♀, USA, California, Mariposa Co., Foresta Rd., 1.1 mi [1.7 km] SSW of Eagle Peak 580 m, 5.v.2004, Griswold leg., at *Clarkia unguiculata*, *Eriodictyon californicum*, K. T. Huntzinger det. (NPIC); ♂, USA, California, Tulare Co., Kern River, 3.v.1996, Griswold leg., *Eriodictyon* sp., T. Griswold det. (NPIC); ♂, USA, California, Tuolumne Co., Cherry Creek, 28.v.1996, Griswold leg., *Clarkia* sp., T. Griswold det. (NPIC).

***Protohalonia amoena* (Zavortink, 1982) comb.n.**

Tetralonia venusta ssp. *venusta*, in part; Timberlake 1961: 209–12.
Synhalonia venusta ssp. *venusta*, in part; Timberlake 1969: 1–76.
Synhalonia amoena Zavortink, 1982: 19–25.
Eucera (*Synhalonia*) *amoena*; Michener 2000: chapter 112.

Holotype ♂, '7 mi [11.2 km] W Havasu | Lake San | Bernardino Co. | CAL[ifornia] 21 April 69', 'Larrea tridentata | 0520-0550 PST | T. J. Zavortink 690421-1A', 'HOLOTYPE | Synhalonia amoena Zavortink 1982', 'California Academy of Sciences | Type No. 14880' (CAS). – Paratype ♀, 'ARIZ[ona] Yuma Co | Salome 22 mSE', VI-73 | G. E. Bohart', 'Larrea', 'Synhalonia | cressoniana | Ckll. | det. W. E. LaBerge', 'Paratype | Synhalonia | amoena | T. J. Zavortink| 1982', 'Native Bee Survey | USDA, Logan, Utah | BBSL515306' (NPIC). – ♂, ♀, USA, California, Inyo Co., Marble Canyon Dunes, North East side, 9.v.2000, Andrus, Griswold & Janjic leg., at *Psorothamnus polydenius*, T. Griswold det. (NPIC); 3♂, ♀, USA, California, Inyo Co., Eureka Dunes, N of Creosote, 8.v.2000, 5:45-6:45, Griswold leg., at *Larrea tridentata*, R. Andrus det. (NPIC); ♀, USA, California, Inyo Co., Eureka Valley, Dry Well site, 7.v.2000, 18:30, Janjic & Griswold leg., T. Griswold det. (NPIC); 2♂, ♀, USA, Nevada, Clark Co., Grand Gulch Rd. 22 air mi [35.4 km] S of Mesquite, 11/21.v.1983, Parker leg., T. Griswold det. (NPIC); ♀, USA, Nevada, Clark Co., Riverside 11/21.v.1983, Parker leg., T. Griswold det. (NPIC); ♂, ♀, USA, Arizona, Yuma Co., 22 mi [35.4 km] SE of Salome, 31.iv.1973, at *Larrea divaricata* [*L. tridentata*], T. Griswold det. (NPIC); ♀, USA, Arizona, Yuma Co., 22 mi SE of Salome, vi.1973, Bohart leg., at *Larrea* sp. [*L. tridentata*], T. Griswold det. (NPIC).

3.6. Natural history

It has been assumed that species of *Protohalonia* are host plant specialists (oligoleges) depending on pollen of Onagraceae. *Protohalonia venusta* has been considered as a specialist of *Camissonia* Link, 1818 (Hurd 1979 and references therein) but analyses of the scopal pollen loads of this species reveal that some *P. venusta* collected a significant amount of pollen of *Larrea* Cavanilles, 1800 (Zygophyllaceae) (Zavortink 1982; A. Dorchin, unpublished data) in line with the evaluation of *P. venusta* as a generalist in studies of *Larrea* pollinators (Minckley et al. 1999; Cane et al. 2006). *Protohalonia carinata* has been considered an oligolege of *Clarkia* Pursh, 1813 (Hurd 1979 and references therein). *Protohalonia amoena* is polylectic, collecting pollen from *Camissonia*, *Larrea*, and *Parkinsonia* Linnaeus, 1753 (Fabaceae: Caesalpinioideae) (Zavortink 1982). The genus *Protohalonia* is vernal, the season of activity is between March and July. All species are matinal and vespertine, *P. venusta* and *P. amoena* collecting at flowers from an hour before sunrise into the early morning, with a second phase of activity observed in the late afternoon until after sunset, as late as 21:00 hours (Linsley et al. 1964; Zavortink 1982). The foraging activity of *P. carinata* appears similar but less extreme, as the species is active as early as 6:18 a.m., shortly after the first *Clarkia* blooms open and again in the late afternoon and evening (MacSwain et al. 1973). Our morphological character analyses indicate that the ocelli in *Protohalonia* species is relatively large, suggesting an adaptation to early matinal activity, although it is not as large as in some other known matinal or crepuscular bees. Our measures found the size of the lateral ocellus changes gradually across species of the *Eucera* complex, with the lateral ocellus greater than the antennal socket only in the *Xenoglossa*-group of *Eucera* (*Xenoglossa*) (the subgenus *Xenoglossa* s.str. in Michener 2007) and in *E.* (*Cemolobus*), while about as large in *Simanthedon* and in the outgroup genus *Martinapis*.

3.7. Distribution

Protohalonia is restricted to the southwestern USA and Baja California, Mexico. *Protohalonia venusta* and *P. amoena* are recorded from arid regions of the Mojave, Sonoran, and Chihuahuan Deserts, and the Great Basin. *Protohalonia amoena* is distributed from New Mexico to Inyo County, California, and southern Nevada; *P. venusta* from western Arizona west to Inyo County, California, (where mixed series of these two species were sometimes taken) and Baja California, and north to southern Oregon. *Protohalonia carinata* is known from cismontane parts of California south to Baja California in Mexico (Ascher & Pickering 2017; Timberlake 1969).

3.8. Phylogenetic analyses

Parsimony analysis of the morphological dataset with equal weights resulted in two most parsimonious trees with minimum length of 854 steps (CI = 0.33; RI = 0.53). The strict consensus calculated for the two trees (Fig. 35) recovered *Protohalonia* as a monophyletic group with strong support (BSP = 6; BS = 93), sister to the genus *Eucera* (*sensu* Dorchin et al. 2018). *Protohalonia* + *Eucera* formed a sister group to a clade that consisted *Martinapis* + *Simanthedon*, but support values for these relationships and for all other basal nodes were minimal (BSP = 1 or 2; BS < 50). Within the genus *Protohalonia*, *P. carinata* appeared as sister to *P. amoena* + *P. venusta*, but this latter clade was weakly supported (BSP = 1) (Fig. 35). The relationships among the various lineages of *Eucera* were generally similar to the ones previously recovered, with the subgenera *Peponapis*, *Xenoglossa*, *Cemolobus*, *Synhalonia*, and *Eucera* s.str. derived from a paraphyletic assemblage that comprise the subgenera *Tetralonia* and *Xenoglossodes* (Fig. 35). Odd placement of some species groups within *Eucera* (e.g., *Cubitalia*-group of *Eucera* s.str.) is not dealt with here, as the present study was not designed for resolving such low-level relationships. A more detailed account of *Eucera* phylogeny and its classification to subgenera is provided in Dorchin et al. (2018).

Our molecular phylogeny recovered *Protohalonia* as a monophyletic group with maximal support (BS = 100 in Fig. 36). It placed *Protohalonia* as sister to *Simanthedon*, and *Protohalonia* + *Simanthedon* as sister to a monophyletic *Eucera* with weak to moderate support (BS = 75 and 69, respectively). The analysis of the Opsin dataset alone resulted in a slightly different topology: *Simanthedon* sister to *Eucera*, and *Simanthedon* + *Eucera* sister to *Protohalonia*, but the former relationship was weakly supported (BS = 69). In analysis of COI alone the relationships between the three genera were unresolved. Contrary to morphological analyses, *Martinapis* was part of a separate clade, sister to the *Eucera* complex.

Relationships within *Protohalonia* differed from those recovered by the morphological analysis with *P. venusta* and *P. carinata* forming a strongly supported clade (BS = 96), sister to *P. amoena* also in single gene analyses of each Opsin and COI. Finally, most *Eucera* subgenera recognized by Dorchin et al. (2018) comprised strongly supported monophyletic groups, namely *Tetralonia*, *Peponapis*, *Xenoglossa*, and *Syntrichalonia*, but *Synhalonia* and *Eucera* s.str. as well as different lineages of the paraphyletic *Xenoglossodes* each received lower support (BS = 26 – 48).

Analysis of the combined molecular and morphological dataset recovered the relationships between the *Eucera* complex genera: *Protohalonia* + *Simanthedon* sister to *Eucera* (BS = 83 for both relationships) with similar topology and higher support values compared to the phylogeny based on molecules alone (Fig. S1). Changes in the position of the *Eucera* subgenera included *Cemolobus* sister to *Xenoglossa* + *Peponapis*, and *Synhalonia* arising from a paraphyletic *Eucera* s.str. (Fig. S1).

3.9. Ancestral state reconstruction

Mapping morphological characters onto our molecular phylogeny tree failed to recover unique synapomorphies for *Protohalonia* (Fig. S2); rather, six character state combinations were found to be unique within the Eucerini, and help to delimitate the new genus in both the female and male (see Diagnosis in 3.1., and see below). Our ancestral state reconstruction showed *Protohalonia* possesses a combination of derived character states and plesiomorphies shared with both lineages of the *Eucera* complex and taxa considered more distantly related such as *Martinapis*, *Melissodes*, and *Svastra* (Table 1). Examples of traits shared only with some *Eucera* complex taxa are (plesiomorphic states follow in parentheses): 1. six maxillary palpomeres (five or less palpomeres); 2. unbranched scopal hairs (Fig. 13) (branched scopal hairs); and 3. conspicuous basolateral marginal projection on S6 of male (Fig. 28) (inconspicuous basolateral marginal projection). In contrast, medial process on S7 of male with abundant short setae (Fig. 30) (inconspicuous, absent, or with setae of different form) is a trait of *Protohalonia* shared only with some outgroup taxa; and simple posterolateral carina of S6 of male (Fig. 28) (posterolateral carina converging with anterior carina) is shared with outgroup taxa plus *Simanthedon* (as well as with *Eucera* (*Xenoglossa*) although the loss of anterior carina is probably secondary in that taxon).

Ancestral state analyses based on ML indicated strong support values of 0.97 – 0.99 proportional likelihood for the following diagnostic character states of the genus *Protohalonia* (plesiomorphic states follow in parentheses; results not presented): 1. Clypeus of female strongly irregularly rugosopunctate (Figs. 7, 8) (at most weakly rugose); anterior lobe of lateral process of male S7 strongly folded as seen in ventral view (Figs. 29, 31) (not folded, simple or otherwise modified); male S8 dorsally pubescent (Fig. 32) (bare or with hairs restricted to apical margin).

Lastly, our ancestral state analysis also identified some diagnostic traits of *Protohalonia* as apomorphies (Table 2), although not all the character states listed in Table 2 were included in our character matrix. A unique synapomorphy supporting the sister relationships of *P. venusta* and *P. carinata* (Fig. S2) recovered in molecular and combined analyses is the narrowly rounded pygidial plate of the male (Fig. 26) (the plesiomorphic states being broadly rounded or obtusely truncate pygidial plate). The pygidial plate of *P. amoena* is variable; it is usually more broadly rounded but some specimens examined in this study had a pygidial plate approaching the unique condition observed in the other *Protohalonia* species.

3.10. List of new homonyms

Relegating a number of genera to subgenera within an expanded genus *Eucera*, our recently proposed classification (Dorchin et al. 2018) has resulted in five new homonyms, and a sixth homonym existing prior to our revisions of the *Eucera* complex, still remaining unresolved. It seems appropriate to propose here new (or available) replacement names to resolve these new homonyms, as follows.

Eucera (*Peponapis*) *atrata* (Smith, 1879) (*Melissodes atrata* Smith, 1879, by original designation) is a junior secondary homonym of *Eucera* (*Synhalonia*) *atrata* Klug, 1845. The name *Eucera atratula* Dalla Torre, 1896, proposed as a replacement name, is available for this species and is reestablished as a valid name (**stat.r.**).

Eucera (*Eucera*) *fasciata* Risch, 1999 is a junior homonym of *Eucera* (*Tetralonia*) *fasciata* (Smith, 1854). The name *Eucera propecineraria* Dorchin (**nom.n.**) is proposed. The adjective "prope" from Latin (meaning "near") is combined with the name *cineraria*, pointing to the close morphological similarity to the valid species *Eucera cineraria* Eversmann, 1852.

Eucera (*Eucera*) *friesei* Risch, 2003 is a junior homonym of *Eucera* (*Tetralonia*) *friesei* (Meade-Waldo, 1914). The name *Eucera rischi* Dorchin (**nom.n.**) is proposed in honor of the taxonomist Stephan Risch, who described the species and has contributed important studies on the taxonomy of Palearctic eucerine bees.

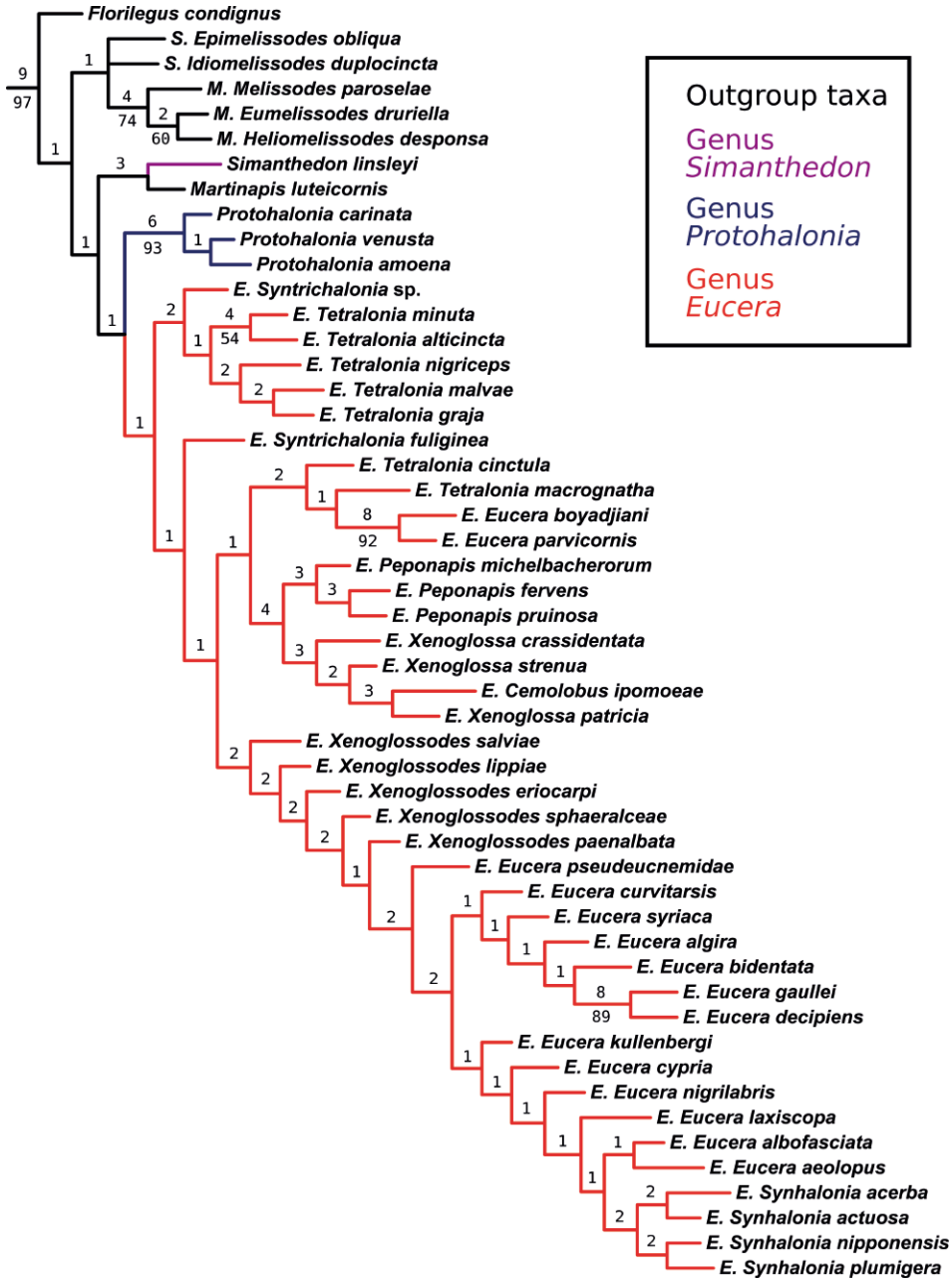

Fig. 35. Strict consensus of two most parsimonious trees found in parsimony analysis of the morphological dataset (854 steps long under equal weights; CI = 0.33; RI = 0.53). Branch support values above branches are Bremer supports (BSP, 12,000 trees, cut 0), those below branches are bootstrap values (BS, 1000 replicates). Outgroup taxa from the tribe Ancylaini have been removed and the branch leading to Eucerini has been modified for better graphic representation. Taxonomy follows Dorchin et al. (2018).

Eucera (*Tetralonia*) *paulyi* (Eardley, 2001) (*Tetraloniella paulyi* Eardley, 2001 by original designation) is a junior homonym of *Eucera* (*Tetralonia*) *paulyi* (Eardley, 1989). The name *Eucera eardleyi* Dorchin (**nom.n.**) is proposed in honor of the research entomologist Connal D. Eardley, who described the species and has contributed numerous studies on the systematics, ecology, and conservation of African bees.

Eucera (*Eucera*) *penicillata* Risch, 1997 is a junior homonym of *Eucera* (*Tetralonia*) *penicillata* (Friese, 1905). The name *Eucera sinufascia* Dorchin (**nom.n.**) is proposed. The nouns "sinu" and "fascia" from Latin (meaning "curved" and "band", respectively) are combined in reference to the band or tuft of hairs on sternite 5 of the male that is typical to the *Pteneucera* group of species, and which is sinuate or curved in this species.

Eucera (*Xenoglossodes*) *fasciata* (LaBerge, 1970) (*Pectinapis fasciata* LaBerge, 1970, by original designation) is a second junior homonym of *Eucera* (*Tetralonia*) *fasciata* (Smith, 1854) listed above. The name *Eucera labergei* Dorchin (**nom.n.**) is proposed in honor of the systematist Wallace E. LaBerge, who described the species and whose substantial contribution to the taxonomy and systematics of American bees has enabled this study.

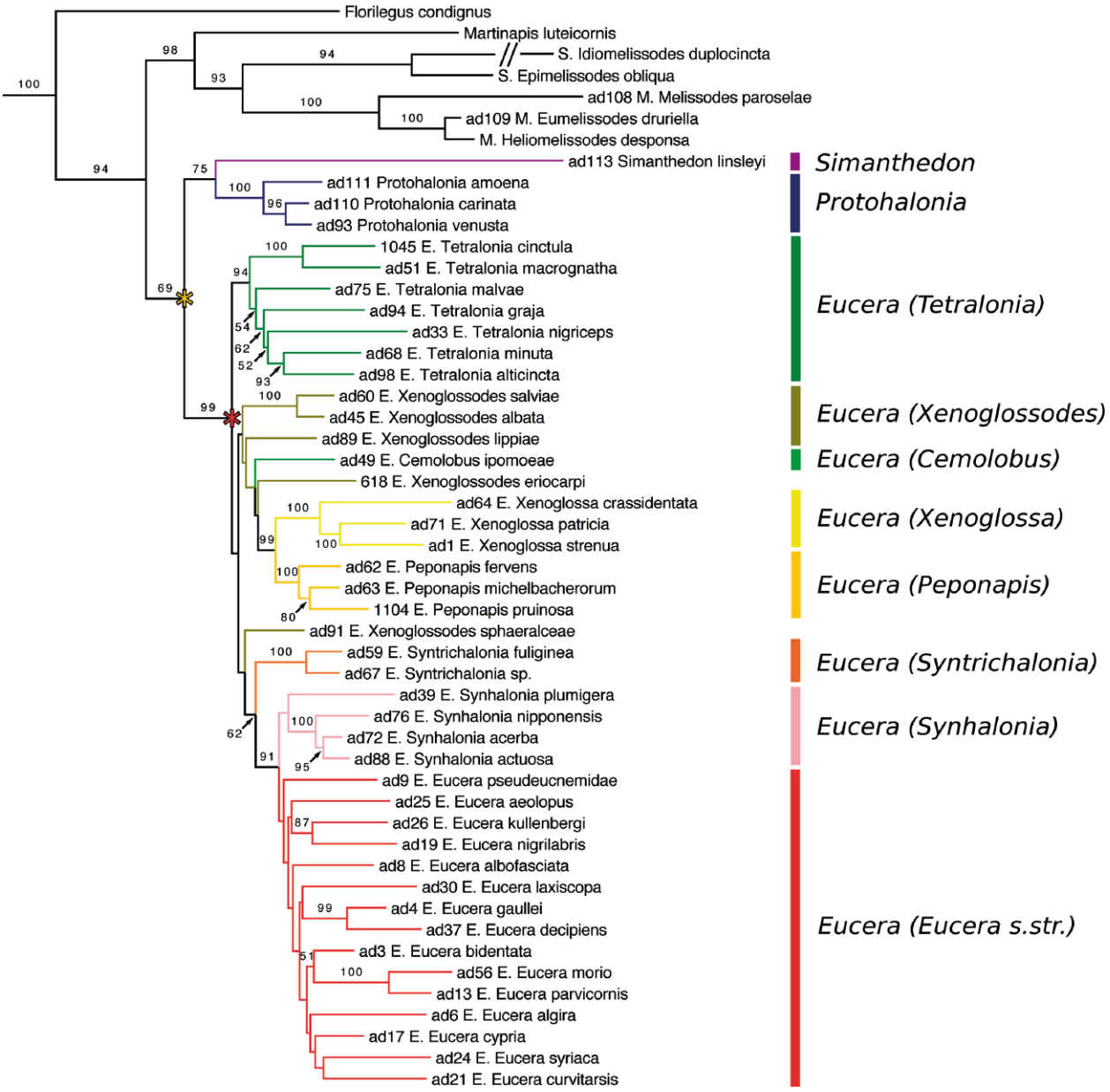

Fig. 36. Best tree found in maximum likelihood analyses of the molecular matrix partitioned by codon position, with the significantly heterogeneous third position of COI excluded; branch support values are bootstrap values (only values ≥ 50%) based on 1000 bootstrap replicates. Taxon names preceded by sample numbers correspond to Table S1 (see Electronic Supplement file 4). Outgroup taxa from the tribe Ancylaini have been removed and the branches leading to Eucerini, and to *Svastra* (*Idiomelissodes*), which represents a long branch, have been modified for better graphic representation. Node corresponding to the *Eucera* complex indicated with a yellow asterisk. Node corresponding to the genus *Eucera* indicated with a red asterisk. Taxonomy follows Dorchin et al. (2018).

4. Discussion

4.1. Characteristics of *Protohalonia* and phylogenetic relationships with its relatives

Results from our morphological, molecular, and combined phylogenies are largely congruent with those of Dorchin et al. (2018). The morphological analyses in that study placed *Protohalonia* in a clade comprising *Martinapis*, *Simanthedon*, and the *Eucera* subgenus *Syntrichalonia*, as sister to the remaining *Eucera* lineages (Dorchin et al. 2018). Our current morphological analysis also recovered a clade *Martinapis* + *Simanthedon* closely related to a clade comprising all *Protohalonia* species, but showed that these two former clades consisted of successive sister groups to a monophyletic *Eucera* (Fig. 35). Our molecular and combined analyses recovered the same generic relationships previously found in the *Eucera* complex, but support for *Protohalonia* + *Simanthedon* was stronger and support for the *Eucera* complex as a whole was weaker (Fig. 36). Altogether, our results reflect greater phylogenetic disparity between genera of the *Eucera* complex, namely *Simanthedon*, *Protohalonia*, and *Eucera*, than has been emphasized so

Table 1. Diagnostic traits of the genus *Protohalonia* Dorchin **gen.n.** and their distribution among related genera and subgenera. Apomorphies are compared with plesiomorphic character states within the Eucerini as indicated by an ancestral state analysis; autapomorphies of *Protohalonia* (Fig. S2) are marked with an asterisk; character numbers refer to the morphological matrix based on Dorchin et al. (2018) (see Electronic Supplement file 1), and taxon names are according to their classification. Cases of inapplicability are marked with (—).

Trait	Parallelism within the *Eucera* complex	Parallelism outside the *Eucera* complex
Apomorphies		
Six maxillary palpomeres (2*)	*Tetralonia* (minus *Eucara*-grp.), *Xenoglossodes* (partim), *Peponapis* (*Eopeponapis*-grp.), *Synhalonia*, *Eucera* s.str.	—
Clypeus moderately protuberant (12)	*Simanthedon*, *Tetralonia* (*Eucara*-grp.), *Cemolobus*, *Xenoglossa*, *Peponapis*, *Synhalonia*, *Eucera* s.str.	—
Malar area linear (18)	*Tetralonia*, *Xenoglossodes*, *Syntrichalonia*, *Eucera* s.str. (minus *Agatheucera*-grp. and *Cubitalia*-grp.)	*Eumelissodes*
Compound eyes with inner margin parallel sided (9) (Figs. 4–6)	*Simanthedon*, *Eucera* s.l.	*Epimelissodes*, *Heliomelissodes*
Female scopal hairs unbranched (48) (Fig. 13)	*Simanthedon*, *Synhalonia*, *Eucera* (minus *Pteneucera*-grp.)	—
Male basolateral marginal projection of S6 conspicuous (79*) (Fig. 28)	*Tetralonia* (*Glazunovia*-grp.), *Xenoglossodes* (partim), *Xenoglossa* (*Xenoglossa*-grp.), *Peponapis* (*Eopeponapis*-grp.), *Synhalonia*, *Eucera* s.str.	—
Gonocoxa with patch of sclerotized setae posteromedially (106)	*Tetralonia* (*Glazunovia*-grp.)	*Epimelissodes*
Spatha posterolateral angle curved mesad, acute (115)	*Simanthedon*, *Xenoglossodes*, *Synhalonia*, *Eucera* s.str.	—
Penis valve inner margin with conspicuous anteromedial lobe as seen in posterior view (118)	*Cemolobus*, *Synhalonia*, *Eucera* s.str.	*Epimelissodes*
Plesiomorphies		
Mesosoma and metasoma with long pubescence (64) (Fig. 16)	*Simanthedon*, *Syntrichalonia*, *Synhalonia*, *Eucera* s.str.	*Florilegus*, *Eumelissodes*, *Martinapis*
Male posterolateral carina of S6 simple, not converging with anterior carina (81) (Fig. 28)	*Simanthedon*, *Xenoglossa*	*Martinapis*, *Svastra*, *Melissodes*
Male medial process of S7 elaborate, elongated, curved apicomesad then apicolaterad (90) (Figs. 29, 31)	*Simanthedon*, *Eucera* s.str. (partim)	*Martinapis*
Male medial process of S7 ventrally setose on distal portion (91) (Fig. 30)	—	*Martinapis*, *Epimelissodes*, *Heliomelissodes*, *Eumelissodes*
S8 apical lobes divided by conspicuous emargination (96) (Fig. 32)	*Tetralonia*, *Xenoglossodes* (partim), *Cemolobus*, *Syntrichalonia*	*Florilegus*, *Martinapis*
Gonostylus gently arcuate in lateral view (107) (Fig. 34)	*Tetralonia* (minus *Eucara*-grp.), *Xenoglossa*	*Florilegus*, *Matinapis*, *Svastra*
Penis valve dorsolateral margin inconspicuously folded mesad (119)	*Simanthedon*, *Tetralonia* (*Eucara*-grp.), *Eucera* s.str. (*Agatheucera*-grp., *Cubitalia*-grp.)	*Martinapis*, *Melissodes*, *Idiomelissodes*

far. In particular, they highlight the position of *Protohalonia* as an early diverging, distinct lineage.

The six unique character state combinations we list in the diagnosis of the new genus (see in 3.1.) comprise informative structural character states that help delineate *Protohalonia* within the *Eucera* complex and the tribe Eucerini in general. The combination of plesiomorphic and apomorphic character states exhibited by species of *Protohalonia* corresponds with its phylogenetic position and shows it shares different suites of traits with both taxa within the *Eucera* complex as well as more distantly related genera such as *Martinapis* (see in 3.9. and Table 1). For example, some derived character states shared with *Eucera* (*Synhalonia*) are the unbranched scopal hairs of the female (albeit finer), the six segmented maxillary palpus, and the well-developed basolateral marginal projection of S6 of the male (Fig. 28). It is probably due to these conspicuous external characters that long supported the placement of *Protohalonia* within *Synhalonia* (Michener 2000; Timberlake 1961, 1969; Zavortink 1982), while less conspicuous plesiomorphies such as the simple linear carina of S6 (Fig. 28), the elaborate S7 of the male (Figs. 29, 31), and the gently arcuate gonostylus of the male (Fig. 34) (the latter two are hidden in the metasoma in repose), were largely overlooked by previous authors (see in 1.).

4.2. Characteristics of *Protohalonia* species and phylogenetic relationships among them

Both morphological and molecular analyses indicate a close relationship among the three *Protohalonia* species (see in 3.8.). Our morphological analysis confirms Zavortink's (1982) conclusions that *P. amoena* and *P. venusta* are closely related and that *P. carinata* is more distantly related to both these species (Fig. 35). In addition to the conspicuously darker vestiture of the female, the structures of the female's maxillary stipes and hairs ventrally on the mesosoma, and the male's antennae are morphological characteristics setting *P. carinata* apart from both other species (Table 2). In contrast to the morphological analysis, our molecular analysis placed *P. amoena* as sister to a group comprising *P. venusta* + *P. carinata* (Fig. 36), a topology that was supported by other structural characters, including one unique synapomorphy (Table 2). It may be possible that the unique morphological traits exhibited by *P. carinata* are simply autapomorphies reflecting adaptation to certain habitat and host plant species (see in 4.3). It is noteworthy that *P. carinata* is a probable specialist on the pollen of *Clarkia* in the plant family Onagraceae, one of the host

Table 2. Diagnostic traits of species of the genus *Protohalonia* Dorchin **gen.n.** Character states identified as apomorphies (Fig. S2) are indicated in parentheses and a unique autapomorphy is marked with an asterisk. Character numbers refer to the morphological matrix (see 2.1. for details).

Character	*P. venusta*	*P. carinata*	*P. amoena*
Female clypeus	Strongly rugusopunctate (Fig. 7), angulate anteriorly in profile (Fig. 10)	Strongly rugusopunctate (Fig. 7), angulate anteriorly in profile (Fig. 10)	Coarsely rugusopunctate (Fig. 8), strongly angulate anteriorly in profile (Fig. 11)
Male clypeus	Rounded, protuberance > 0.75 × compound eye width	Rounded, protuberance > 0.75 × compound eye width	Weakly angular, submedially depressed, protuberance ~ 0.7 × compound eye width
Male antennae	Rounded in cross section, filiform, ~ 3 × as long as compound eye, with distal flagellomere uniformly broad	Weakly laterally compressed, weakly crenate, ~ 3.6 × as long as compound eye, with distal flagellomere transversely constricted preapically (6)	Rounded in cross section, filiform, ~ 3 × as long as compound eye, with distal flagellomere uniformly broad
Male, maximum length of first antennal flagellomere	> 0.8 × as long as second (Fig. 22)	0.6 – 0.7 × as long as second (5) (Fig. 23)	> 0.8 × as long as second (Fig. 22)
Female stipital comb teeth	Separated by < 1 basal diameter of adjacent comb teeth	Separated by ~2 basal diameters of adjacent comb teeth (27)	Separated by < 1 basal diameter of adjacent comb teeth
Female hair color of face	Light (Fig. 4)	Dark (Fig. 5)	Light (Fig. 6)
Female hairs posteromedially on underside of mesosoma	Apically bent unbranched hairs	Ordinary branched hairs (38)	Apically bent unbranched hairs
Female, density of posterior hair band on T2	Moderately dense, not concealing underlying integument medially	Sparse, not concealing underlying integument throughout	Dense, concealing completely underlying integument
Female scopal hair color	Pale grey to brown on outer tibia, brownish ferruginous to black on inner side of basitarsus	Brown to black on both sides of tibia and basitarsus	Cream whitish on outer tibia, bright ferruginous on inner side of basitarsus
Male outer ramus of hind claw	Slightly longer than inner ramus (Fig. 24)	Distinctly longer than inner ramus (Fig. 25)	Slightly longer than inner ramus (Fig. 24)
Male pygidial plate	Narrowly rounded apically, with complete lateral carina (68*) (Fig. 26)	Narrowly rounded apically, with complete lateral carina (68*) (Fig. 26)	More broadly rounded apically, with lateral carina weakly interrupted before apex (Fig. 27)
Male posterior lobe of lateral process of S7	Large, weakly elevated, strongly carinate with short apicolateral spine (Fig. 29)	Large, moderately elevated, strongly carinate with short apicolateral spine (Fig. 29)	Small, strongly elevated, with faint carina and long, hooked apicolateral spine (Fig. 31)
Male distal arm of medial process of S7	Curved dorsally apicomesad from a sclerotized dark angle, produced apically into a broad oval lobe (Fig. 29)	Curved dorsally apicomesad from a sclerotized dark angle, produced apically into a broad oval lobe (Fig. 29)	Curved ventrally apicomesad from a sclerotized dark angle, produced apically into greatly enlarged lobe (Fig. 31)
Male gonocoxa, orientation of posterodorsal projection	Posteromesad	Posteromesad	Posterodorsad (104)
Male gonostylus basally	Distinctly broadened	Slightly broadened	Slightly broadened

plant families used by the pollen generalists *P. venusta* and *P. amoena*. These results are in line with studies on other groups of bees showing that specialist species often use the same host plants also used by generalist species (Müller 1996; Sipes & Tepedino 2005: Sedivy et al. 2008, 2013). Further study, especially the inclusion of additional sequence data is expected to resolve the phylogenetic relationships within *Protohalonia* when fresh DNA samples for all these uncommon species becomes available.

4.3. Homoplasious characters and their use in diagnosis of *Protohalonia*

Diagnostic traits of *Protohalonia* (see in 4.1.) that also appear homoplasiously in *Eucera* include unbranched scopal hairs and six maxillary palpomeres (Table 1), both of which represent functional traits: scopal hairs are used in pollen transport and maxillary palpi in chemical sensory. Such functional traits may be more easily attained through convergent loss or gain and are more likely to appear homoplasiously across lineages (Litman et al. 2016; Trunz et al. 2016; Rightmyer et al. 2013; Dorchin et al. 2018). Indeed, the same characters vary frequently in state also among the different subgenera of *Eucera* (e.g., in *Eucera* (*Xenoglossodes*): LaBerge 2001; *Eucera* (*Tetralonia*): Risch 2001; *Eucera* (*Eucera* s.str.): Risch 2003; and *Eucera* (*Peponapis*): Michener 2007).

The scopal hairs of *Protohalonia*, although unbranched, were noted as unusually fine and dense in previous revisions (Timberlake 1961, 1969; Zavortink 1982) as well as in this study. Their fine scopal hairs were long suspected as an adaptation for collecting the small pollen grains of some plants in the family Onagraceae, on which these bees were thought to be specialized. *Protohalonia venusta* was considered a specialist on the pollen of *Camissonia claviformis* (Torrey & Frémont) Raven, 1964 (Linsley et al. 1963), and *P. carinata* a specialist on the pollen of *Clarkia unguiculata* Lindley, 1837 (MacSwain et al. 1973). The association of scopal structure to pollen collection behavior was recently investigated in detail by Portman & Tepedino (2017), who demonstrated that the unbranched, and sometimes denser scopal hairs of Onagraceae bee specialists are an adaptation for transporting dry pollen. They suggested that the sticky vis-

cin threads typical to Onagraceae pollen bind the pollen in the scopa, replacing the floral nectar used by related moist-transporting species to bind the pollen (Portman & Tepedino 2017). Our observations are in line with the conclusions from that study, including transport of dry pollen in *Protohalonia* in contrast to moistened pollen in some *Eucera*, in which the scopal hairs are coarser (Dorchin et al. 2018).

Another suspected functional trait of this group is the color of vestiture. The lighter vestiture differentiating females of *P. amoena* and *P. venusta* from those of *P. carinata* (see in 4.2.), may reflect an adaptation to the warm desert habitats of these two former species. It is replaced by darker vestiture in *P. carinata*, possibly because this species inhabits the temperate cismontane regions of California (Ascher & Pickering 2017; Timberlake 1969). Thus, lighter vestiture that help reduce the absorption of sun radiation and prevent excessive heating, may result from convergence rather than homology. Interestingly, a female *P. carinata* collected in Baja California, where populations of *P. carinata* and *P. venusta* are found in close geographical proximity, had an unusually lighter vestiture (Timberlake 1969) approaching the color variation observed in *P. venusta*, and may thereby support this hypothesis. On the other hand, we could not find a comparable geographical pattern to explain the wide color variation observed in the metasomal vestiture of females *P. venusta* (from almost entirely white to almost entirely black; Timberlake 1961; and see description of the female in 3.1.).

Despite the incongruity of the characters discussed here in phylogenetic inference in our study, they could still be useful when combined with other phylogenetically informative characters in diagnosis of the genus *Protohalonia* (Table 1).

4.4. Conclusions

It has been the tradition of bee systematists to recognize large genera further divided into multiple subgenera (e.g., *Megachile* Latreille, 1802, *Andrena* Fabricius, 1775, and *Lasioglossum* Curtis, 1833; see Michener 2007). Consequently, the discovery of new genera is not common in bees but may emerge from phylogeny-based revisions, especially when including species-poor, early diverging lineages. One such genus is *Xenofidelia* Packer, 2017, the second genus in the small Megachilidae subtribe Neofideliini that was recently discovered in the Northern Atacama Desert of Chile (Packer et al. 2017). The genus *Protohalonia*, described as new in this study is an example of a group that was relatively well studied but repeatedly overlooked by previous authors (Timberlake 1969; Zavortink 1982; Michener 2000) until reinvestigated in a phylogenetic context (Dorchin et al. 2018). The present study calls for further investigations into the phylogenetic and systematic relationships between *Protohalonia* and its closest relatives. Especially when fresh DNA becomes available for *Protohalonia* and the monotypic genus *Simanthedon*, the use of additional molecular markers should shed light on their relationships with such genera as *Martinapis*, which appears closely related in morphological analyses.

5. Acknowledgements

This research was supported by a fellowship granted to A. Dorchin by the Israeli Taxonomy Initiative (ITI). Sequencing of *P. carinata* and *P. amoena* was generously funded and performed at G. Kahila Bar-Gal's laboratory of molecular evolution, The Hebrew University of Jerusalem. We thank N.D. Penny, the California Academy of Sciences, for providing us access to type material, P. Oboyski, the Essig Museum of Entomology, University of California at Berkeley, for providing additional specimens of *Protohalonia venusta*, and C.L. Ritner, the USDA ARS Bee Biology & Systematics Laboratory, Utah State University, and E. Ockermüller, the Upper Austrian State Museum, Biologiezentrum, Linz, Austria, for taking images. We also thank Z.M. Portman, the Native Bee Lab, Department of Entomology, University of Minnesota, C.J. Praz, the Institute of Biology, University of Neuchatel, an anonymous reviewer, and the journal editors for providing helpful comments that improved this paper. The authors declare no conflict of interest.

6. References

Ascher J.S., Pickering J. 2017. Discover Life Bee Species Guide and World Checklist (Hymenoptera: Apoidea: Anthophila). – http://www.discoverlife.org/20/q?search=Apoidea (accessed 17.8.2017)

Bremer K. 1994. Branch support and tree stability. – Cladistics **10**: 295–304.

Cane J.H., Minckley R.L., Kervin L.J., Williams N.M. 2006. Complex responses within a desert bee guild (Hymenoptera: Apiformes) to urban habitat fragmentation. – Ecological Applications **16**: 632–644.

Danforth B.N. 1999. Phylogeny of the bee genus *Lasioglossum* (Hymenoptera: Halictidae) based on mitochondrial COI sequence data. – Systematic Entomology **24**: 377–393.

Dorchin A., López-Uribea M.M., Praz C.J., Griswold T., Danforth B.N. 2018. Phylogeny, new generic-level classification, and historical biogeography of the *Eucera* complex (Hymenoptera: Apidae). – Molecular Phylogenetics and Evolution **119**: 81–92.

Goloboff P.A., Farris J.S., Källersjö M., Oxelman B., Ramírez M.J., Szumik C.A. 2003. Improvements to resampling measures of group support. – Cladistics **19**: 324–332.

Goloboff P.A., Farris J.S., Nixon K.C. 2008. TNT, a free program for phylogenetic analysis. – Cladistics **24**: 774–786.

Hurd P.D. Jr. 1979. Superfamily Apoidea. Pp. 1741–2209 in: Krombein K.V., Hurd P.D. Jr., Smith D.R., Burks B.D. (eds), Catalog of Hymenoptera in America North of Mexico. Vol. 2. – Smithsonian Institution Press, Washington.

Inkscape Development Team 2017. Inkscape: a professional quality vector graphics software. – https://inkscape.org.

Katoh K., Standley D.M. 2013. MAFFT multiple sequence alignment software version 7: improvements in performance and usability. – Molecular Biology and Evolution **30**: 772–780. http://dx.doi.org/10.1093/molbev/mst010.

Kimball S., Mattis P., GIMP Development Team 2016. GIMP: GNU Image Manipulation Program. – https://www.gimp.org.

LaBerge W.E. 1957. The genera of bees of the tribe Eucerini in North and Central America. – American Museum Novitates **1837**: 1–44.

LaBerge W.E. 2001. Revision of the bees of the genus *Tetraloniella* in the New World. – Illinois Natural History Survey Bulletin **36**: 63–162.

Linsley E.G., MacSwain J.W., Raven P.H. 1963. Comparative behavior of bees on Onagraceae, I. *Oenothera* bees of the Colorado Desert. – University of California Publications in Entomology **33**: 1–24.

Linsley E.G., MacSwain J.W., Raven P.H. 1964. Comparative behavior of bees and Onagraceae, III. *Oenothera* bees of the Mojave desert. – University of California Publications in Entomology **33**: 59–98.

Litman J.R., Griswold T., Danforth B.N. 2016. Phylogenetic systematics and a revised generic classification of anthidiine bees (Hymenoptera: Megachilidae). – Molecular Phylogenetics and Evolution **100**: 183–198.

MacSwain J.W., Linsley E.G., Raven P.H., Thorp R.W. 1973. Comparative behavior of bees and Onagraceae, IV. *Clarkia* bees of the western United States. – University of California Publications in Entomology **70**: 1–80.

Maddison W.P., Maddison D.R. 2015. Mesquite: a modular system for evolutionary analysis. Version 3.02. – http://mesquiteproject.org.

Michener C.D. 2000. The Bees of the World. – The Johns Hopkins University Press, Baltimore, Maryland.

Michener C.D. 2007. The Bees of the World. 2nd edn. – The Johns Hopkins University Press, Baltimore, Maryland.

Miller M.A., Pfeiffer W., Schwartz T. 2010. Creating the CIPRES science gateway for inference of large phylogenetic trees. In: Proceedings of the Gateway Computing Environments Workshop (GCE) (New Orleans, Los Angeles, November 14, 2010).

Minckley R.L., Cane J.H., Kervin L., Roulston T.H. 1999. Spatial predictability and resource specialization of bees (Hymenoptera: Apoidea) at a superabundant, widespread resource. – Biological Journal of the Linnean Society **67**: 119–147.

Müller A. 1996. Host-plant specialization in western palearctic anthidiine bees (Hymenoptera: Apoidea: Megachilidae). – Ecological Monographs **66**: 235–257.

Nixon K.C. 2002. WinClada. – Published by the author, Ithaca, New York. – http://www.cladistics.com.

Packer L., Litman J.R., Praz C.J. 2017. Phylogenetic position of a remarkable new fideliine bee from northern Chile (Hymenoptera: Megachilidae). – Systematic Entomology **42**: 473–488.

Patton W.H. 1879. Generic arrangement of the bees allied to *Melissodes* and *Anthophora*. – Bulletin of the United States Geological and Geographical Survey of the Territories **5**: 471–479.

Portman Z.M., Tepedino V.J. 2017. Convergent evolution of pollen transport mode in two distantly related bee genera (Hymenoptera: Andrenidae and Melittidae). – Apidologie **48**: 461–472.

Praz C.J., Packer L. 2014. Phylogenetic position of the bee genera *Ancyla* and *Tarsalia* (Hymenoptera: Apidae): a remarkable base compositional bias and an early Paleogene geodispersal from North America to the Old World. – Molecular Phylogenetics and Evolution **81**: 258–270. http://dx.doi.org/10.1016/j.ympev.2014.09.003.

Rightmyer M.G., Griswold T., Brady S.G. 2013. Phylogeny and systematics of the bee genus *Osmia* (Hymenoptera: Megachilidae) with emphasis on North American *Melanosmia*: subgenera, synonymies and nesting biology revisited. – Systematic Entomology **38**: 561–576.

Risch S. 2001. *Tetralonia trimera* – eine neue *Tetralonia*-Art mit drei Maxillarpalpengliedern (Hymenoptera: Apidae). – Linzer Biologische Beiträge **33**: 949–953.

Risch S. 2003. Die Arten der Gattung *Eucera* Scopoli 1770 (Hymenoptera, Apidae). Die Untergattungen *Stilbeucera* Tkalců 1979, *Aopeucera* Tkalců 1984, und *Hemieucera* Sitdikov and Pesenko 1988. – Linzer Biologische Beiträge **35**: 1241–1292. www.zobodat.at/pdf/LBB_0029_1_0555-0580.pdf.

Sedivy C., Praz C.J., Müller A., Widmer A., Dorn S. 2008. Patterns of host-plant choice in bees of the genus *Chelostoma*: the constraint hypothesis of host-range evolution in bees. – Evolution **62**: 2487–2507.

Sedivy C., Dorn S., Widmer A., Müller A. 2013. Host range evolution in a selected group of osmiine bees (Hymenoptera: Megachilidae): the Boraginaceae−Fabaceae paradox. – Biological Journal of the Linnean Society **108**: 35–54.

Sipes S.D., Tepedino V.J. 2005. Pollen-host specificity and evolutionary patterns of host switching in a clade of specialist bees (Apoidea: *Diadasia*). – Biological Journal of the Linnean Society **86**: 487–505.

Stamatakis A. 2014. RAxML version 8: a tool for phylogenetic analysis and postanalysis of large phylogenies. – Bioinformatics **30**: 1312–1313. http://dx.doi.org/10.1093/bioinformatics/btu033.

Swofford D.L. 2002. PAUP 4.0 Phylogenetic Analysis using Parsimony (* and other methods). – Sinauer Associates, Sunderland Massachusetts, USA.

Timberlake P.H. 1961. A new species of *Tetralonia* from the deserts of California and Nevada. – Pan-Pacific Entomologist **37**: 209–212.

Timberlake P.H. 1969. A contribution to the systematics of North American species of *Synhalonia*. – University of California Publications in Entomology **57**: 1–76.

Trunz V., Packer L., Vieu J., Arrigo N., Praz C.J. 2016. Comprehensive phylogeny, biogeography and new classification of the diverse bee tribe Megachilini: Can we use DNA barcodes in phylogenies of large genera? – Molecular Phylogenetics and Evolution **103**: 245–259.

Zavortink T.J. 1982. A new species of *Synhalonia* in the *venusta* group (Hymenoptera: Anthophoridae). – The Wasmann Journal of Biology **40**: 19–25.

Electronic Supplement Files

at http://www.senckenberg.de/arthropod-systematics

File 1: dorchin&al-eucerinibees-asp2018-electronicsupplement-1.pdf — Morphological character matrix.

File 2: dorchin&al-eucerinibees-asp2018-electronicsupplement-2.pdf — **Fig. S1**: Best tree found in maximum likelihood analysis of the combined molecular and morphological matrix.

File 3: dorchin&al-eucerinibees-asp2018-electronicsupplement-3.pdf — **Fig. S2**: Best tree found in maximum likelihood analyses of the molecular phylogeny model with morphological characters mapped onto the tree branches.

File 4: dorchin&al-eucerinibees-asp2018-electronicsupplement-4.pdf — **Table S1**: Taxa included in the phylogenetic analyses and their subgeneric affiliation, locality data, and voucher depository.

File 5: dorchin&al-eucerinibees-asp2018-electronicsupplement-5.pdf — **Table S2**: Primer sequences and PCR conditions for primer pairs.

Zoobank Registrations

at http://zoobank.org

Present article: http://zoobank.org/urn:lsid:zoobank.org:pub:93316AAA-69CE-420F-846E-555E52BB2FE1

***Protohalonia* Dorchin, 2018:** http://zoobank.org/urn:lsid:zoobank.org:act:F6B0B3EF-2A5B-4482-A6C6-C0670D449D3E

***Protohalonia amoena* (Zavortink, 1982):** http://zoobank.org/urn:lsid:zoobank.org:act:AFFE0179-5985-4A1E-9D90-8AC8E8388581

***Protohalonia carinata* (Timberlake, 1961):** http://zoobank.org/urn:lsid:zoobank.org:act:EFF49AF2-43DE-4DF2-A0A4-831AB15B0E11

***Protohalonia venusta* (Timberlake, 1961):** http://zoobank.org/urn:lsid:zoobank.org:act:306AF2F9-1EBC-4ED6-AC6B-8D6E76DD8383

***Eucera atratula* Dalla Torre, 1896:** http://zoobank.org/urn:lsid:zoobank.org:act:C21A7D09-F0D1-4A57-8E55-80B98554F1B7

***Eucera propecineraria* Dorchin, 2018:** http://zoobank.org/urn:lsid:zoobank.org:act:E4201948-1AE4-456B-919C-2246E7EFB831

***Eucera rischi* Dorchin, 2018:** http://zoobank.org/urn:lsid:zoobank.org:act:782726B9-2101-4ABF-981C-78998ECA44C2

***Eucera sinufascia* Dorchin, 2018:** http://zoobank.org/urn:lsid:zoobank.org:act:7A047F58-340A-4929-9B31-D7D6F23FB401

***Eucera labergei* Dorchin, 2018:** http://zoobank.org/urn:lsid:zoobank.org:act:0BF1166E-87A4-433B-89D4-D44548D980DD